Acta Oceanol. Sin., 2025, Vol. 44, No. 3, P. 35–56
https://doi.org/10.1007/s13131-024-2442-4

Water masses in the Southern Ocean: Variability, trends, and drivers

Zhaomin Wang[1], Ying Li[2, 3, 4], Jiuxin Shi[5], Zhaoru Zhang[6, 7, 8], Chengyan Liu[1], Meng Zhou[6, 7, 8, 9*], Zexun Wei[2, 3, 4*]

[1] Southern Marine Science and Engineering Guangdong Laboratory (Zhuhai), Zhuhai 519080, China

[2] First Institute of Oceanography, and Key Laboratory of Marine Science and Numerical Modeling, Ministry of Natural Resources, Qingdao 266061, China

[3] Laboratory for Regional Oceanography and Numerical Modeling, Qingdao Marine Science and Technology Center, Qingdao 266237, China

[4] Shandong Key Laboratory of Marine Science and Numerical Modeling, Qingdao 266061, China

[5] Physical Oceanography Laboratory, Ocean University of China, Qingdao 266100, China

[6] Key Laboratory of Polar Ecosystem and Climate Change, Ministry of Education and School of Oceanography, Shanghai Jiao Tong University, Shanghai 200240, China

[7] Shanghai Key Laboratory of Polar Life and Environment Sciences, Shanghai Jiao Tong University, Shanghai 200240, China

[8] Shanghai Frontiers Science Center of Polar Science, Shanghai Jiao Tong University, Shanghai 200240, China

[9] Key Laboratory for Polar Science, Polar Research Institute of China, Shanghai 200240, China

Received 27 August 2024; accepted 9 December 2024

© Chinese Society for Oceanography and Springer-Verlag GmbH Germany, part of Springer Nature 2025

Abstract

The Southern Ocean is a critical component in the Earth system by dominating the global heat and anthropogenic carbon uptake and supplying heat to melt the largest ice sheet. Variability and changes in the water masses of the Southern Ocean are thus important to the global energy and water cycles, carbon cycling, and sea-level change. In this article, we review the recent progress on understanding the variability and changes in the four major water masses in the Southern Ocean, including Subantarctic Mode Water, Antarctic Intermediate Water, Circumpolar Deep Water and Antarctic Bottom Water. Subantarctic Mode Water and Antarctic Intermediate Water show statistically significant strong circumpolar shoaling, warming, and density reductions since 1970s, indicating that signals of global warming have entered the interior ocean. Meanwhile, strong regional variability of Subantarctic Mode Water and Antarctic Intermediate Water responding to surface buoyancy forcing and westerly winds is attracting more attention. Circumpolar Deep Water is an important modulator of heat content and nutrient concentrations on continental shelves around Antarctica and has made significant contributions to the basal melting of Antarctic ice shelves. Since the late 1950s, a long-term freshening trend in Antarctic Bottom Water in the Ross Sea and its downstream region has been observed and is mainly attributed to the accelerated basal melting of ice shelves in West Antarctica. The shrinking of Antarctic Bottom Water in the Weddell Sea during 1992–2020 has also been revealed and is attributed to reduced sea ice production over the southern Weddell continental shelf related to the Interdecadal Pacific Oscillation and the variability in the Amundsen Sea Low. Though significant advances have been achieved, there is an urgent need to enhance and improve both observations and model performances for better understandings and projections of the formation, transformation, and transport of the water masses in the Southern Ocean.

Foundation item: The Independent Research Foundation of Southern Marine Science and Engineering Guangdong Laboratory (Zhuhai) under contract Nos SML2023SP201 and SML2021SP306; the Natural Science Foundation of Guangdong Province of China under contract No. 2024A1515012717; the Initial Research Foundation of Southern Marine Science and Engineering Guangdong Laboratory (Zhuhai) under contract Nos 313021004, 313022009, and 313022001; the National Natural Science Foundation of China under contract No. 41706225; the National Key R&D Program of China under contract No. 2018YFA0605701; the Impact and Response of Antarctic Seas to Climate Change under contract No. IRASCC 1-02-01B; the Shenlan Program funded by Shanghai Jiao Tong University under contract No. SL2020MS021; the fund from Shanghai Frontiers Science Center of Polar Research.

*Corresponding author, E-mail: meng.zhou@sjtu.edu.cn; weizx@fio.org.cn

Key words Southern Ocean, Subantarctic Mode Water, Antarctic Intermediate Water, Circumpolar Deep Water, Antarctic Bottom Water, variability, trend, driver

Citation Wang Zhaomin, Li Ying, Shi Jiuxin, Zhang Zhaoru, Liu Chengyan, Zhou Meng, Wei Zexun. 2025. Water masses in the Southern Ocean: Variability, trends, and drivers. Acta Oceanologica Sinica, 44(3): 35–56, doi: 10.1007/s13131-024-2442-4

1 Introduction

The Southern Ocean comprises waters between the Antarctic continent and its northern boundary at 60°S or traditionally the Polar Front (PF). In this review paper, the Southern Ocean refers to the waters extending to the south of the subtropical gyres or Subtropical Front (STF) (Fig. 1). Four major water masses, including Subantarctic Mode Water (SAMW), Antarctic Intermediate Water (AAIW), Circumpolar Deep Water (CDW), and Antarctic Bottom Water (AABW), are formed or transformed in the Southern Ocean. Through its unique connections to the other major oceans and interactions with the atmosphere and cryosphere, the Southern Ocean is a critical component in the Earth system. Both observations and model simulations indicate that the Southern Ocean dominates the global oceanic heat uptake (Roemmich et al., 2015; Frölicher et al., 2015). The Southern Ocean also constitutes a major carbon reservoir in the Earth system (Sarmiento, 2006), and hence plays a key role in the global carbon cycle. In the modern era, the Southern Ocean is critically important in taking up anthropogenic carbon from the atmosphere (Frölicher et al., 2015; Sarmiento et al., 2004). The Southern Ocean also has a dominant influence on the Antarctic ice sheet, which contains ice of approximately 57.9 m global sea-level equivalent (Morlighem et al., 2020). Thus, variability and changes in the water masses in the Southern Ocean are critical to the global energy and water cycles, carbon cycling, and sea-level change.

SAMW is located in the three Southern Hemisphere ocean basins and distributed between the Subantarctic Front (SAF) and STF, featured by relative uniform properties vertically and hence by low Potential Vorticity (PV) (McCartney, 1977). SAMW origins from the formation of a deep and thick mixed layer in austral wintertime, driven by surface ocean heat loss and enhanced deep convection. The physical processes of the SAMW subduction from the mixed layer into the permanent pycnocline are associated with momentum, heat and freshwater fluxes driven by air-sea interactions, Ekman pumping, diapycnal mixing, and cross-frontal water exchanges. SAMW shows distinct properties dominated by its generation zone in different oceanic basins. SAMW in each basin is then advected northward, which is the major part of the upper limb of the global overturning circulation, ventilating the lower thermocline waters in the Southern Ocean (Herraiz-Borreguero and Rintoul, 2011; Sloyan and Rintoul, 2001). Consequently, SAMW has a vital contribution to the global heat, salt, nutrients, and carbon budget. Understanding the dynamics of SAMW is critical to properly

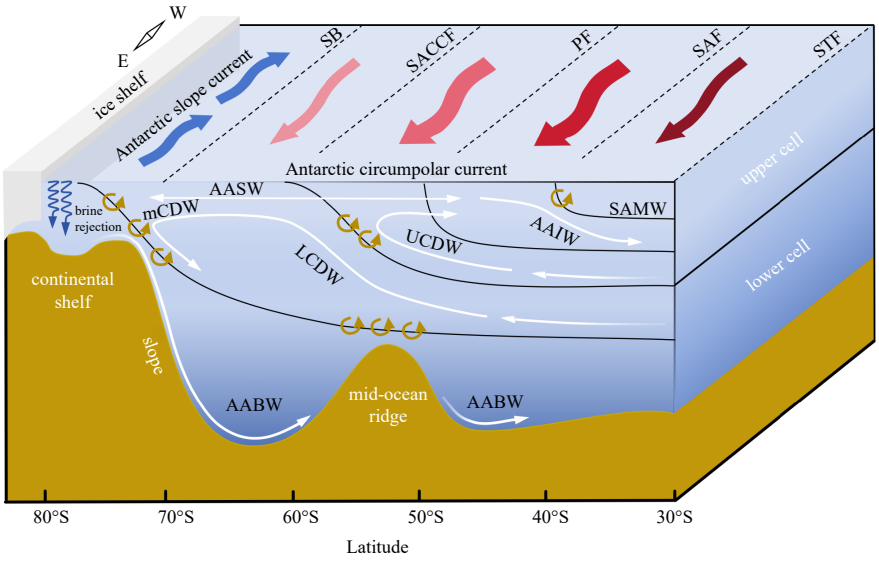


Fig. 1. Schematic of major water masses and overturning circulation in the Southern Ocean. AABW: Antarctic Bottom Water; AAIW: Antarctic Intermediate Water; AASW: Antarctic Surface Water; LCDW: Lower Circumpolar Deep Water; mCDW: modified Circumpolar Deep Water; PF: Polar Front; SACCF: South Antarctic Circumpolar Current Front; SAMW: Subantarctic Mode Water; SAF: Subantarctic Front; SB: Southern Boundary of Antarctic Circumpolar Current; STF: Subtropical Front; UCDW: Upper Circumpolar Deep Water.

projecting global climate changes.

Denser than SAMW, AAIW is identified by a low salinity layer at about 500 m to 1 500 m depth in the subtropical gyres of the Southern Hemisphere and the tropics of the Pacific and Atlantic (Talley et al., 2011). AAIW is mostly originated from the Antarctic Surface Water (AASW) subducting across SAF (Deacon, 1937) and the SAMW formed by winter deep convection in the Subantarctic Zone (McCartney, 1977). AAIW then spreads to the north with the subtropical gyres as a gradually weakening salinity-minimum layer (McCartney, 1977; Talley, 1996). Part of AAIW finally enters the north Atlantic to balance deeper export of the North Atlantic Deep Water (NADW) (Gordon et al., 1992). The formation and subduction of AAIW constitute the upper branch of the global overturning circulation (Sloyan and Rintoul, 2001), by which AAIW plays a vital role in Earth's climate system in effecting the global-scale uptake, storage and oceanic transport of heat, salt and carbon (Li et al., 2023b).

CDW is the largest water mass by volume transported by the Antarctic Circumpolar Current (ACC), which can approach the Antarctic continental shelves by the proximity of the ACC to the shelf. CDW can upwell to a depth comparable to the shelf and then intrude onto shelf regions via troughs, eddies, topographic Rossby waves, and buoyancy-driven baroclinic currents (Klinck and Dinniman, 2010; St-Laurent et al., 2013; Liu et al., 2017; Wang et al., 2024). Once reaching ice shelves, the heat supplied by CDW could cause significant ice shelf basal melting, which may further result in thinning and calving of ice shelves that buttress glaciers to suppress ice flows into the ocean (Dinniman et al., 2012; Cook et al., 2016). In this sense, CDW plays an important role in Antarctic ice sheet mass balance and thus the global sea level rise. CDW is also a nutrient-rich water mass that can promote the biological production of Antarctic shelf ecosystems (Zhang et al., 2020).

AABW is the densest water mass occupying the abyss in the Southern Ocean. AABW mainly originates from Dense Shelf Water (DSW) on the Antarctic continental shelf. Strong brine rejection in winter leads to the formation of High Salinity Shelf Water (HSSW) in the coastal polynyas. The mixing between HSSW and other shelf waters generates DSW (Foldvik et al., 2004; Orsi and Wiederwohl, 2009). During its cascading in the slope regions, DSW mixes with its ambient waters and sinks to the abyssal oceans to form AABW. AABW occupies much of the world ocean floor by its northward spreading. The formation and transport of AABW drive the lower limb of the global overturning circulation (Lumpkin and Speer, 2007; Talley, 2013), supplying oxygen (Gordon, 2013) to the abyssal ocean and storing heat and carbon in the abyssal ocean for centuries or longer (de Lavergne et al., 2017; Holzer et al., 2021). The variability of AABW greatly influences global climate through its connection to the circulation in the Atlantic, Pacific, and Indian Ocean basins on a variety of time scales. The formation of AABW also affects the nutrient cycling and primary production on the Antarctic continental shelf and even globally (Marinov et al., 2006). Variability and changes in the AABW formation are thus able to influence the global overturning circulation, carbon cycling, and marine ecosystem, on time scales from decadal to millennial (Sigman and Boyle, 2000; Ferrari et al., 2014; Marzocchi and Jansen, 2019).

The water masses mentioned above are closely linked together by the Southern Ocean overturning circulation (Fig. 1). Under the forcing of surface winds and major topographic features in the Southern Ocean, the upwelling of CDW brings deep water to the surface and poleward along tilted density surfaces. A significant portion of the upwelled water is transformed to lighter water by precipitation and sea ice melt and is then pushed equatorward by westerly winds to produce SAMW and AAIW, forming the upper cell of the Southern Ocean overturning circulation. The poleward portion of the upwelled water further intrudes onto the continental shelf around Antarctica and is transformed to DSW by cooling and sea ice formation. The transformation of DSW during its sinking in the slope regions leads to the formation of AABW, driving the lower cell of the Southern Ocean overturning circulation. In this article, we review the recent progress on understanding the spatial patterns and temporal variations of these water masses and major driving processes, to facilitate the understanding of the changes in the Southern Ocean and their global impacts.

2 Subantarctic Mode Water

SAMW is generated by subduction of the winter deep mixed layer into the interior ocean, which leads to a weak-stratified and well-ventilated subsurface water mass. Connecting the surface with the interior ocean, SAMW contributes to renewing the lower thermocline waters in the three subtropical gyres of the Southern Hemisphere. Therefore, main forcings such as air-sea momentum and buoyancy fluxes, diapycnal mixing, and mesoscale eddies play important roles in the generation and evolution of SAMW (Fig. 2). However, the relative impact of each process on the SAMW formation is expected to exhibit variability across different formation sites (Iudicone et al., 2011). In the past, observations were much sparse in the Southern Ocean, which limited our knowledge of the variation of the SAMW, and even led to conflicting views (Bryden et al., 2003; Naveira Garabato et al., 2009; Herraiz-Borreguero and Rintoul, 2010). Based on the continuous observations and the improved climate models, recent studies have significantly quantified the formation, distribution, variability of SAMW in recent years (e.g., Herraiz-Borreguero and Rintoul, 2011; Gao et al., 2018; Qiu et al., 2024).

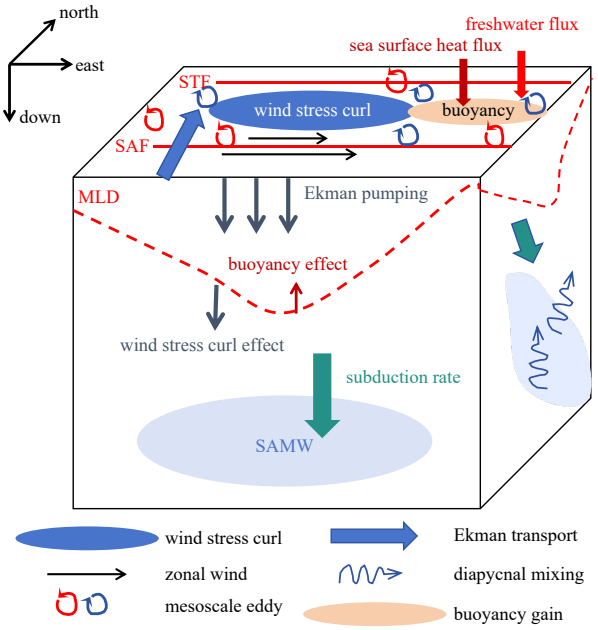


Fig. 2. Schematic of Subantarctic Mode Water (SAMW) formation and variation mechanisms in the Southern Ocean [modified from Wang et al. (2022)]. Here air-sea buoyancy flux mainly includes heat flux and freshwater flux. SAF: Subantarctic Front; STF: Subtropical Front.

2.1 *Spatial pattern and formation processes of SAMW*

SAMW is widely found at intermediate depths, within 200 m to 800 m in the Southern Ocean. SAMW has different temperature, salinity, and density characteristics in the Indian, Pacific, and Atlantic sectors, followed by an unevenly spatial distribution of this water mass in the Southern Ocean, with thicker and cooler SAMW in the eastern Indian and Pacific sectors but thinner and warmer SAMW in the western Indian and Atlantic sectors (Herraiz-Borreguero and Rintoul, 2011).

The SAMW formation regions are highly related to the winter mixed layer depth (MLD) distribution from west-north to east-south in each sector. The strongest subduction rate and the largest volume of SAMW are found in the southern Indian Ocean and the southern Pacific Ocean (Sallée et al., 2006; Cerovečki et al., 2013). A deeper MLD leads to a larger subduction rate of mode water. It is worth noting that the local MLD maxima are located around major topographic features where the flow is steered southward. Thick SAMW layers are hence generated around major topographic features (Aoki et al., 2007). Meanwhile, numerous subduction processes are highly related to the MLD, which is dominated by wind forcing, buoyancy flux, diapycnal mixing and mesoscale eddies. The MLD has significant positive correlation with wind stress curl but negative correlation with the buoyancy flux (Wang et al., 2022). The wind stress drives cold surface water northward from the south of the SAF (Gao et al., 2018). The formation of SAMW is dominated by the buoyancy loss that drives the subduction of SAMW from the mixed layer into the permanent pycnocline. Local subduction and diapycnal mixing are demonstrated to be responsible for the SAMW volume variations in the South Indian and South Pacific Oceans (Portela et al., 2020; Li et al., 2021). Mesoscale eddies are incredibly active in the Southern Ocean, and eddy activities could be enhanced by rough topography. Mesoscale features influence the properties of SAMW, which can lead to cold or warm anomalies in SAMW (Herraiz-Borreguero and Rintoul, 2010).

It is found that air-sea fluxes, density advection, and diapycnal mixing have similar contributions to SAMW formation and destruction by analyzing the results from the Southern Ocean State Estimate (SOSE) (Cerovečki et al., 2013). It is, however, necessary to identify the relative impact of each process at each formation site (Iudicone et al., 2011).

SAMW formation has also been found to be strongly correlated with changes in sea ice meltwater area in the northern Ross Sea and northern Amundsen/Bellingshausen seas, because of meridional sea ice advection into the formation region (Sanders et al., 2023). During the past decades, the Southern Annular Mode (SAM) has shown a significant trend of shift toward its positive phase, which leads to the poleward shift and enhancement of westerly winds (Sallée et al., 2010). The SAMW formation and transformation are modulated by the SAM-induced MLD changes and the outcrop zone affected by wind stress changes.

2.2 *Temporal variations of SAMW and drivers*

Due to the limited observational data, previous studies treated SAMW in the Southern Ocean as a whole to analyze the variation of SAMW, which is obviously meaningful for estimating the impact of SAMW on heat and carbon exchanges. Using the definition of SAMW in a certain density range, the variations of thickness, volume, and heat content were quantified in many studies (e.g., Gao et al., 2018; Meijers et al., 2019; Portela et al., 2020; Qu et al., 2020). During the Argo era, it has been shown that SAMW was thickened, deepened, and warmed significantly, and its spatial variation was highly correlated with the change of wind stress (Gao et al., 2018; Qu et al., 2020). Numerical models were used to prove the above changes in SAMW volume and showed an increase of 11% between 1950 and 2017 (Jing and Luo, 2021). More studies define SAMW by PV minimum in each ocean basin to provide much greater detail in SAMW spatial variation (e.g., Hong et al., 2020; Xu et al., 2021). Besides, extra constraints such as density, temperature, and salinity were applied to identify SAMW (Li et al., 2021; Wang et al., 2022).

The volume variation of SAMW could remain inconsistent within different density layers in the same region. For example, a 10% volume reduction mostly occurs in

the dense SAMW at 1 026.8–1 026.9 kg/m^3, while a small increase occurs in the lighter SAMW at 1026.6–1026.8 kg/m^3 in the southern Indian Ocean during 2004–2018 (Hong et al., 2020), which is caused by weakening Mascarene High (MH) (also called Indian Ocean subtropical high) and westerly wind anomaly. Due to the seasonal migration of the outcrop window, the formation and destruction of SAMW shift over a large meridional range. The strongest formation occurs equatorward of the SAF in wintertime because of surface ocean heat loss, and occurs in the polar gyres in spring and summer through the freshening of water (Cerovečki and Mazloff, 2016). For example, the changes of Southeast Indian SAMW spreading into the subtropical gyre or ACC are different in three different density layers, which is associated with changes of formation regions due to the meridional shift of the outcrop zone (Qiu et al., 2024).

Due to subduction and ventilation processes, periodic temporal variation of formation and evolution of SAMW are sensitive to the atmosphere-ocean interaction. As mentioned above, seasonal, interannual, and decadal SAMW variability are not spatially uniform across the Southern Ocean (e.g., Cerovečki et al., 2019; Portela et al., 2020).

Both observational and modeling studies have demonstrated the important roles of buoyancy forcing and wind stress in driving the subduction through the mixed layer into the permanent pycnocline. The seasonal variations of SAMW are governed by both buoyancy fluxes and wind forcing (Gao et al., 2018). Wind stress curl and buoyancy fluxes that affected SAMW variations are related to anomalies in the westerly winds. However, wind stress curl dominate the changes in SAMW in the Indian sector, while buoyancy fluxes have more important effect in the Pacific and Atlantic sectors (Wang et al., 2022). By separating SAMW into two components within the mixed layer and in the interior ocean, Li et al. (2021) quantified that SAMW volume in the mixed layer dominated the seasonal variability of SAMW volume, with contributions from air-sea buoyancy fluxes (45%), entrainment (35%), and northward Ekman transport across the Subantarctic Front (10%).

Recent efforts have focused on investigating the links between SAMW variability and large-scale climate phenomena. The interannual variability in SAMW is mostly affected by the variations in buoyancy fluxes (Cerovečki et al., 2019; Xu et al., 2021). The SAMW volume changes in the Indian Ocean are controlled by surface forcing related to MH with a lag of about three years (Hong et al., 2020). During the Global Warming Hiatus period (1998–2016), the MH intensity has been confirmed to be weakened (Vidya et al., 2020). And then associated surface buoyancy flux, Ekman pumping and westerly winds changed the SAMW volume variability. Composites of mixed layer depth anomalies during positive and negative SAM phases show that the MLDs have different responses to wind anomalies over the SAMW subduction regions in the Indian and Pacific Oceans (Sallée et al., 2010). For SAMW in the Pacific Ocean, low-frequency variability of wind speed is dominated mainly by the Interdecadal Pacific Oscillation and to a lesser extent by the SAM (Jing et al., 2024).

It was observed that the SAMW in the Southern Ocean became warmer, fresher, lighter, and less ventilated during 2004–2019, but the core of the SAMW remained at a constant depth (Xu et al., 2021). This is due to a balance between increased wind stress curl and increased buoyancy fluxes. The lightening of SAMW and reducing ventilation are mainly due to increased surface buoyancy forcing due to warming, while the stronger westerly winds play a weaker role and slow down the lightening trend. The temporal trend of SAMW also show different features in different ocean basins (Wang et al., 2022). Results show that the subduction rate of SAMW tends to increase in the South Pacific but to decrease in the Southern Indian Ocean during 1958–2016 (Qiu et al., 2021). The volume of SAMW in the Southern Indian Ocean decreased by 10% from 2004 to 2018 (Hong et al., 2020), and the shrinking mainly occurred in the denser lower layer, owing to surface forcing changes caused by weakening MH and westerly winds. However, the volume of the less dense upper SAMW increases slightly (Hong et al., 2020). During the same period, SAMW showed increasing trends in temperature and salinity (Zhang et al., 2021), and the trends were also different between the upper and lower layers. The volume of the warmer and saltier lower-density SAMW in the upper layer increased, while the volume of the colder and fresher SAMW in the lower layer decreased. These changes were caused by the deepening of the isopycnal interface of SAMW and were also ultimately attributed to changes in wind and surface buoyancy forcing.

3 Antarctic Intermediate Water

As one of the major water masses discovered at the beginning of the oceanographic survey in the Southern Ocean, AAIW is believed to be formed primarily by circumpolar cross-frontal mixing and subsequent subduction of low-salinity AASW and SAMW according to its circumpolar distribution and its typical core feature of salinity minimum in vertical profiles (e.g., Deacon, 1937). This traditional circumpolar view of AAIW formation had never been doubted until McCartney (1977) noticed that the SAMW formed in the region around southern South America are identical in temperature and salinity to the South Pacific and South Atlantic varieties of AAIW, and suggested that AAIW is formed primarily in the southeast Pacific and Atlantic Ocean sectors of the Subantarctic Zone, as the coldest and freshest variety of SAMW. With more observational evidences, including an oxygen maximum associated with the AAIW core, the view is strengthened that AAIW formation is dominated in the

southeast Pacific Ocean sector while AAIW in the Atlantic and Indian Ocean sectors is derived from advection of the southeast Pacific AAIW through Drake Passage with additional modification in that region (Talley, 1996). The presence of distinctly different AAIWs in the three sectors of the Southern Ocean is attributed to the regional mixings along the AAIW transport path rather than new ventilation (Piola and Georgi, 1982; Hanawa and Talley, 2001).

The controversy about the AAIW formation source origins has never been resolved even after new research methods except for *in situ* observations were applied. The results from an inverse box model reveal both the outcropping of SAMW around the Drake Passage and the circumpolar cross-frontal transport and transformation play important roles in the renewal of AAIW (Sloyan and Rintoul, 2001). Investigation of the intensity and regional variability of the ventilation process confirms that most of the water in the AAIW density class subducts in Drake Passage (Sallée et al., 2010). Most numerical simulations support the local view of AAIW formation (England et al., 1993; Marsh et al., 2000; Saenko et al., 2003), while less models support the circumpolar view (Santoso and England, 2004) or their combination (Sørensen et al., 2001).

Recently, three sub-types of AAIW are identified by applying a machine learning approach to individual Argo profiles (Xia et al., 2022). In addition to the two traditionally known sub-types, the Southeast Pacific AAIW and the circumpolar AAIW, a new sub-type of AAIW formed along the SAF in the South Pacific Ocean is also identified. This unsupervised classification result reflects a complicated pattern of AAIW formation, modification and circulation.

3.1 *Transformation and circulation of AAIW*

As a water mass sandwiched between overlying thermocline and underlying deep water and circulating in both the Southern Ocean and all adjacent subtropical oceans, AAIW is an active member in the closure of the deep and thermocline circulation in the Southern Ocean and/or the adjacent subtropical oceans (Sloyan and Rintoul, 2001). Before subducting into the intermediate layer, surface waters are replenished by upwelling, which constructs a part of the upper branch of the overturning circulation in the Southern Ocean. The circumpolar-averaged circulation shows an upwelling in the AAIW density classes, which is carried north into a zone of dense SAMW subduction (Sallée et al., 2010). A thermodynamic analysis to assess the diabatic processes controlling overturning in the Southern Ocean reveals a seasonal two-stage cold transit in the formation of intermediate water from upwelled deep water (Evans et al., 2018). First, relatively warm and saline deep water is transformed into colder and fresher near-surface winter water via wintertime mixing. Second, winter water warms to form intermediate water through summertime surface heat fluxes.

By quantifying and contrasting the effects of subduction by Ekman pumping and geostrophic flow, eddy-induced subduction, and water mass transformation due to mesoscale and small-scale mixing, the transformation of waters within the AAIW density range (neutral density between 27.25 kg/m^3 and 27.7 kg/m^3) has been quantified (Li et al., 2022). Ekman pumping upwells the denser AAIW into the mixed layer south of PF, which can be advected northward by Ekman transport into the subduction regions of less dense AAIW and SAMW. The subduction of less dense AAIW occurs mainly by lateral advection in the southeast Pacific and Drake Passage as well as eddy-induced flow between SAF and PF. The diapycnal transport from subducted SAMW into the AAIW layer is predominantly by mesoscale mixing near the SAF and vertical mixing in the South Pacific Ocean, while AAIW is further replenished by transformation from upper Circumpolar Deep Water (UCDW) by vertical mixing. The results suggest that the distribution of AAIW is set by its formation due to subduction and mixing, and its circulation eastward along the ACC and northward into the subtropical gyres.

AAIW is a central player in the large-scale inter-basin circulation cells (Fig. 3) associated with the global overturning circulation (Sloyan and Rintoul, 2001). The South Pacific Ocean is one of hot spot regions of AAIW research for the southeast Pacific Ocean and has long been considered as a main source of AAIW (McCartney,

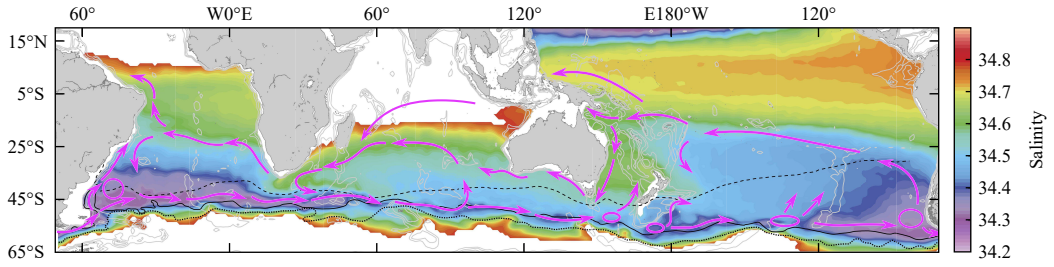


Fig. 3. Salinity at the Antarctic Intermediate Water (AAIW) core (salinity minimum) plotted using Argo data averaged over 2005 to 2020, with a sketch of AAIW formation (purple ellipse) and circulation (purple arrow) according to Gordon et al. (1992), Sloyan and Rintoul (2001), Bostock et al. (2013), Yao and Shi (2017), and Li et al. (2022). Dashed line, solid line, and dotted line indicate Subtropical Front, Subantarctic Front, and Polar Front, respectively, with data from Orsi et al. (1995). Gray lines are depth contours of 1 000 m, 2 000 m, and 3 000 m.

1977). The formation rates of AAIW (defined in a potential density range of 27.06–27.40 kg/m^3) from PF to 20°N in the South Pacific Ocean was quantified as (5.8 ± 1.7) × 10^6 m^3/s based on ChloroFluoroCarbon (CFC) inventories (Hartin et al., 2011). The AAIW produced in the southeast Pacific is then subducted northward into the South Pacific subtropical gyre (Talley, 1996). The resulting low-salinity layer is apparent throughout the Pacific Ocean up to the southern boundary of the subtropical gyre in the North Pacific Ocean (Hanawa and Talley, 2001). The circulation and mixing of AAIW in the South Pacific Ocean were reviewed using evidence from physical and geochemical tracers and Argo float trajectories (Bostock et al., 2013). This study confirms that the main formation region of AAIW is the southeast Pacific Ocean, where fresh, cold, high oxygen, low nutrient, and intermediate waters are created. Then, this AAIW is transported north and mixes with Equatorial Pacific Intermediate Waters. Other two sub-types of AAIW are "Tasman" AAIW found in the Coral and Tasman Seas, and "Southern Ocean" AAIW most likely a mixture of AAIW formed locally at the SAF and AAIW formed along the SAF in the southeast Pacific or Indian oceans and transported by ACC. A transition type between these two sub-types AAIW can be identified in the region east to the Tasmania (Yao and Shi, 2017).

While the less dense AAIW is carried back into the South Pacific subtropical gyre by a regional circulation loop, the denser AAIW is mostly carried away into the Atlantic Basin (Sallée et al., 2010). The South Atlantic AAIW originates from surface waters in northern Drake Passage and the Falkland Current loop (Talley, 1996). An oxygen maximum is associated with the AAIW through much of the South Atlantic Ocean (Hanawa and Talley, 2001). Cool AAIW enters the South Atlantic Ocean and moves northward adjacent to the South American coast with the Malvinas Current, then meets the southward Brazil Current, forming the Brazil–Malvinas confluence, which moves eastward across the Atlantic Ocean as the South Atlantic Current, and then is transported southeastward over the mid-Atlantic ridge (Sloyan and Rintoul, 2001). The North Atlantic thermohaline circulation is closed primarily by intermediate water that enters the Atlantic Ocean through Drake Passage (Gordon et al., 1992; Sloyan and Rintoul, 2001),

There is a significant inter-ocean exchange of AAIW between the South Atlantic and Indian oceans. The South Atlantic water loops back to the Atlantic Ocean within the Indian Ocean, perhaps mostly within the Agulhas recirculation cell of the southwest Indian Ocean (Gordon et al., 1992). Most of the westward flow south of Africa enters the Atlantic Ocean in the Benguela Current (Sloyan and Rintoul, 2001).

AAIW in the Indian Ocean had ever been thought originating from the South Atlantic Ocean (Talley, 1996). CFC and hydrographic data indicate that the most recently ventilated AAIW is observed in a compact anticyclonic gyre west of 72°E for its eastward extent and is deflected and limited by the Kerguelen Plateau (Fine, 1993). Argo data show that the salinity minimum associated with AAIW in the South Indian Ocean is centered on an isopycnal with potential density of 27.2 kg/m^3 and fresh AAIW is injected northward into the subtropical gyre at about 65°–85°E (Wong, 2005).

Tracers are consistent with an inter-ocean flow from the South Pacific Ocean into the Eastern Indian Ocean, similar to the linkage between the South Atlantic Ocean and the Indian Ocean (Fine, 1993). Several currents get together to complete the connection between the South Pacific Ocean and the Indian Ocean, including the East Australia Current in the Southwest Pacific Ocean, the Tasman Leakage, and the Flinders Current in the South Australian Basin, and the extension of Flinders Current in the southeast Indian Ocean (Yao and Shi, 2017).

3.2 *Temporal variations of AAIW*

Long-term trends of AAIW have been identified by comparisons of hydrographic data collected along the World Ocean Circulation Experiment (WOCE) repeat transects since the end of last century.

By comparing historical hydrographic data collected between 1930 and 1980 with trans-oceanic hydrographic transects during 1985–1994 in the Pacific (17°S, 43°S between Tasmania and New Zealand) and Indian oceans (32°S), a coherent basin-wide freshening of AAIW is found and is attributed to the freshening of surface waters in the high latitude Southern Ocean (Wong et al., 1999, 2001).

An analysis of hydrographic data collected along 24°S transect in the South Atlantic Ocean show that AAIW significantly warmed from 1958 to 2009, with a significant salinification from 1958 to 1983 and a subsequent period of smaller change in salinity (McCarthy et al., 2011). Changes in the salinity of AAIW are shown to be linked with the Indian Ocean influence by the increased Agulhas leakage rather than the intensification of the hydrological cycle.

As a choke point, Drake Passage is the most frequently observed region of the Southern Ocean. A time series of the physical and biogeochemical properties during 1969–2005 constructed using 24 transects of measurements across the passage indicates that AAIW had experienced substantial variability on interannual to interdecadal time scales (Naveira Garabato et al., 2009). Changes in AAIW are mainly forced by variability in Winter Water (the minimum temperature layer in AASW) properties resulting from fluctuations in wintertime air-sea turbulent heat fluxes and spring sea ice melting, both of which are linked to predominantly ENSO-driven variations in the intensity of meridional winds to the west of the Antarctic Peninsula. For the interdecadal variability, AAIW underwent a net freshening (by about 0.05) between the 1970s

and the twenty-first century, which were seemingly forced by an interdecadal trend in the SAM and regional positive feedbacks in the air-sea ice coupled climate system.

The availability of Argo data with higher temporal and spatial resolution enhances the studies of AAIW variability. A 50-year (1960–2010) time series reproduced from historical hydrographic data and Argo data confirms that the freshening trend of AAIW at the 32°S transect in the Indian Ocean had persisted into the first decade of the new century (Kobayashi et al., 2012). Using an isopycnal climatology constructed from Argo data to define the modern state of the AAIW core (salinity minimum), the variations of AAIW since the mid-1970s are studied (Schmidtko and Johnson, 2012). The properties at the AAIW core show statistically significant strong circumpolar shoaling (30–50 m/decade), warming (0.05–0.15℃/decade), and density reductions [up to −0.03 (kg·m^{-3})/decade]. These trends are strongest just north of the ACC in the southeast Pacific and Atlantic Oceans and decrease equatorward. Salinity trends for the whole AAIW are generally small, while long-term freshening is found in the southeast Pacific, southwest Atlantic, and south-central Indian Oceans, with salinification south of Africa and Australia. The gridded monthly mean Argo data reveals a basin-scale freshening of AAIW in the South Atlantic during the period from 2005 to 2014, which is also revealed by two repeated transects along 30°S (Yao et al., 2017). A decrease in the transport of Agulhas Leakage accounts for approximately 53% of the observed freshening, while the freshening has been compensated for by a salinity increase of thermocline water, indicating a local hydrological cycle intensification. A latest result using Argo data shows that AAIW (defined in a neutral density range of 27.05 kg/m^3 to 27.75 kg/m^3) has warmed and thinned due to the deepening of lighter isopycnals so that its heat content decreased by 1.4×10^{21} J/a over the Argo era (2005–2020) (Li et al., 2023b). This finding highlights the complexity of the AAIW response to global warming.

Reanalysis data are much helpful for understanding the temporal variations of AAIW. With ocean assimilation data during 1979–2008, Yang and He (2014) investigated the AAIW in the region of Brazil and Malvinas confluence, where locates the maximum anomalies of AAIW decadal variability. They proposed that the local mesoscale eddies may play an important role in triggering this decadal oscillation. In an estimation of the volume change of the interior water masses in the Southern Hemisphere oceans between 2006 and 2015 with reanalysis data (Portela et al., 2020), the AAIW (defined in potential density between the 27.2 kg/m^3 and 27.5 kg/m^3) shows the strongest trend of volume decrease. In a density-spiciness framework, this volume loss can be explained by its negative isopyncal transformation southward of the ACC into the fresher and colder AASW and northward into spicier tropical/subtropical intermediate waters. The results of AAIW volume budget in the Southern Ocean based on an ocean model output show that the diapycnal mixing and the surface buoyancy flux dominates the interannual variation of AAIW in the Indian Ocean and in the Pacific Ocean, respectively (Zhang et al., 2023). The AAIW volume decreased by approximately 7.2% from 1955 to 2017, due to a consistent increase of oceanic buoyancy gain over the outcropping area and, thus, more AAIW being transformed into lighter water.

4 Circumpolar Deep Water

CDW is a warm ($T > 1.5$℃) and saline ($S > 34.6$) water mass occupying the intermediate depth of the Southern Ocean (Talley et al., 2011). It lies between AASW (south of the SAF) or AAIW (north of the SAF) and AABW. CDW can approach the Antarctic continental shelves by the proximity of the ACC to the shelves or by joining the Weddell and Ross gyres. While the Antarctic Slope Current (ASC) acts as a barrier for the CDW to access to the Antarctic continental shelves, on-shelf CDW intrusion can be achieved by several dynamical processes including mesoscale eddies resulting from frontal instability, topographic Rossby waves, baroclinic currents, flow inertia, bottom Ekman transports (Klinck and Dinniman, 2010; St-Laurent et al., 2013; Stewart and Thompson, 2016; Liu et al., 2022; Wang et al., 2024). The intruded CDW then mixes with the shelf waters to form modified CDW (mCDW). The shoreward flow of mCDW can supply significant amount of heat to the base of ice shelves and thus play an important role in the ice shelf basal melting (Depoorter et al., 2013; Nakayama et al., 2014b). The CDW is also a nutrient-rich water mass that can stimulate primary production in the Antarctic shelf ecosystems (Gerringa et al., 2020).

4.1 *CDW in the Southern Ocean and its upwelling pathways*

The CDW can be further classified into two water mass types—the UCDW and the lower CDW (LCDW). The UCDW is featured by high temperature, low oxygen and rich nutrients, which is mainly supplied by the Pacific Deep Water (PDW) and the Indian Deep Water (IDW). The LCDW is distinguished by high salinity that mainly origins from the NADW (Orsi et al., 1999). Combining hydrographic measurements and particle tracking in a high-resolution numerical model, Tamsitt et al. (2017) revealed that deep water enters the ACC from north via deep western boundary currents along continents or topographic ridges and along eastern pathways driven by eddy activities, and then spirals southeastward and upward into the ACC. Upwelling is enhanced when the ACC encounters major topographic features including the Southwest Indian Ridge, Kerguelen Plateau, Macquarie Ridge, Pacific-Antarctic Ridge, and Drake Passage. Tamsitt et al. (2018) further quantified the water mass transformation of the

CDW along its upwelling pathways originating from the three ocean basins based on the eddy-permitting SOSE. While rich eddies at major topographic features can cause rapid water mass transformation, the cumulative transformation along the CDW upwelling trajectories is mainly induced by background mixing.

4.2 *Dynamics of the CDW intrusion onto Antarctic continental shelves*

Mechanisms for the on-shelf intrusion of CDW have been the research foci of water mass studies in the Southern Ocean. Thompson et al. (2018) classified the Antarctic continental shelves into three categories: fresh shelf, dense shelf and warm shelf (Fig. 4). For the fresh shelf, fronts on the slope are featured by density surfaces tilting downward from north to south and intersecting the slope, and CDW has to move across isopycnals to access to the shelf. The dense shelf is characterized by a V-shaped frontal feature that accommodates both the offshore transport of DSW and onshore transport of CDW, and mesoscale turbulence at the interface between the DSW and CDW plays a role in promoting the CDW on-shelf intrusion. For the warm shelf, CDW shoals continuously from the open ocean to the shelf, which is quite favorable for its onshore movement. Klinck and Dinniman (2010) proposed a couple of possible mechanisms for the cross-slope transport of CDW including the following: (1) Ekman transport in the bottom boundary layer, (2) flow inertia in the presence of bathymetry curving onshore, (3) vertical excursion of isopycnals in the Antarctic Slope Front (ASF), (4) instability of the ASC frontal jets, (5) atmospheric forcing such as westerlies that drive upwelling of deep water, (6) circulations driven by the buoyance of ice shelf meltwater.

Submarine troughs are identified as important conduits for the on-shelf intrusion of CDW. Using an idealized eddy-resolving model simulating the dynamics of western Antarctica oceanic processes, St-Laurent et al. (2013) suggested three mechanisms for the CDW onshore movement within submarine troughs: (1) a deep onshore flow driven by the ice shelf basal melting, (2) interaction between the alongshore mean flow and the trough, and (3) interaction between Rossby waves on the continental slope and the trough topography. Based on a realistic high-resolution coupled ocean-sea ice-ice shelf model for Prydz Bay, Liu et al. (2017) identified submarine troughs east of the Four Ladies Bank as an important pathway for the CDW shoreward flows. Liu et al. (2022) proposed three mechanisms governing the CDW intrusion through troughs over fresh shelf regions with an idealized eddy-resolving ocean-ice shelf coupled model, which includes the following: (1) bottom pressure torque, (2) topographic beta effect and (3) topographic Rossby waves. Morrison et al. (2020) found significant correlation of the inflow of CDW to outflow of DSW within troughs on the Antarctic shelf, and attributed such relationship to the fact that the transport of DSW creates cross-trough sea-level gradient inducing onshore geostrophic transport of the CDW. Ong et al. (2024) found intrinsically episodic intrusions of the CDW through canyons on Antarctic shelves using an eddy-resolving isopycnal model simulating the dynamics of East Antarctic marginal seas, which are attributed to the interaction between wind energy input and eddies generated from the ASF.

Eddies play an important role in mediating the cross-slope transport of CDW and the associated heat fluxes. Stewart and Thompson (2016) found that the shoreward CDW transport is significantly modulated by mesoscale and submesoscale eddies, which are mainly generated by instability at the interface between the CDW and DSW with energy supply from buoyancy loss on the continental shelf. Stewart et al. (2018) revealed that eddy stirring along isopycnals is the primary mechanism for shoreward heat transport around Antarctica, which is modulated by tides and surface wind forcing.

A couple of studies revealed the mechanisms for the CDW onshore intrusion by performing vorticity budget analysis for circum-Antarctic or regional shelves. Diagnosis of time-mean vorticity budget based on the SOSE reanalysis product suggests that in the Amundsen Sea, the cross-slope CDW transport is mainly controlled by vorticity input from the wind stress curl at the shelf break (Ro-

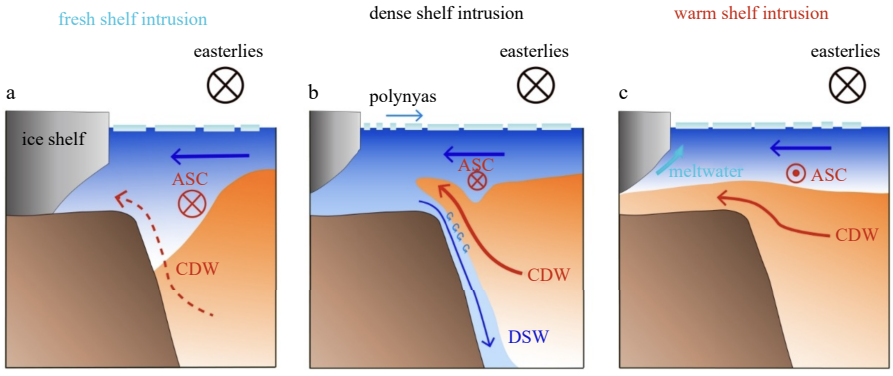


Fig. 4. Schematic illustrating the on-shelf intrusion of the Circumpolar Deep Water (CDW) on the fresh (a), dense (b), and warm (c) continental shelves [modified from Thompson et al. (2018)]. ASC: Antarctic Slope Current, DSW: Dense Shelf Water.

driguez et al., 2016). Based on depth-integrated vorticity budget analysis for circum-Antarctic shelves using simulations from a global eddy-permitting ocean-sea ice model, Palóczy et al. (2020) showed that in the Amundsen Sea, Bellingshausen Sea, and Weddell Sea, the vorticity budget on the shelves is dominated by the topographic Sverdrup balance, which is the balance between surface vortex stretching/squeezing caused by surface Ekman pumping and bottom vortex squeezing/stretching associated with the cross-slope flows. Wang et al. (2024) developed a coupled high-resolution ocean-sea ice-ice shelf model for the Ross Sea and Amundsen Sea, and depth-integrated vorticity balance analysis based on the model simulations reveals that in the Ross Sea the onshore transport of CDW is primarily controlled by the joint effect of baroclinicity and relief term, which results from along-isobath density gradient on the slope between the DSW and the iceshelf meltwater from the Amundsen Sea. On short timescales, the variability of CDW intrusion is demonstrated to be related to topographic Rossby waves (Liu et al., 2022).

4.3 *Temporal variations of the CDW and the forcing mechanisms*

Studies on the temporal variability of CDW are more focused on seasonal and interannual time scales, while the variations at higher frequencies and in the long term under climate change are also revealed. On the seasonal scale, mooring observations detected strong CDW inflows in austral summer and weak inflows in austral autumn in the Ross Sea (Castagno et al., 2017). Using numerical simulations from a coupled high-resolution ocean-sea ice-ice shelf model for the Ross Sea, Wang et al. (2023b) also found strong CDW intrusion in austral summer. Significant correlation exists between the onshore flow of CDW and poleward Sverdrup transport in the open ocean associated with Ekman pumping induced by surface stress curl, such that larger stress curl in summer under low sea ice concentration promotes the upwelling and onshore intrusion of the CDW. Based on mooring observations on the slope of Prydz Bay, Guo et al. (2022) found that prominent CDW intrusion occurs between March and July, which is significantly related to the wind field north of the shelf break and lags the wind variation by about 60 d; poleward shift of the westerlies drives upwelling and shoaling of the CDW and then facilitates its on-shelf intrusion. Gao et al. (2024) observed persistent eddies carrying warm CDW onto the Prydz Bay shelf in mooring measurements and hydrographic section data in 2013–2015; such eddies are more active in summer when westerlies are strengthened, enhancing the CDW upwelling and initiating eddy formation.

On the interannual scale, using long-term data from the Antarctic Marine Life Resources program, Zhang et al. (2020) detected significant, positive correlation between the variation of mCDW extent on the shelf of the northern Antarctic peninsula and the variation of SAM in austral spring, which is caused by the wind variation associated with SAM; the SAM-induced CDW change has significant impacts on the phytoplankton biomass in this region as CDW is a nutrient-rich water mass. With observations obtained during the Chinese National Antarctic Research Expedition in the Dotson-Getz Trough in the summers of 2020 and 2022, Xie et al. (2023) identified strengthening of the CDW onshore intrusion and eastward shift of the intrusion path in 2022, which results from the poleward shift of westerlies that enhances the CDW upwelling on the slope as well as the enhancement of eastward undercurrents that promotes the onshore Ekman transport of CDW in the bottom layer. Chen et al. (2023) found notable relationship between the interannual variations of CDW onshore intrusion in the Ross Sea and eddy kinetic energy on the slope, and demonstrated that eddies play a crucial role in modulating the variations of onshore heat transport toward the Ross Sea shelf.

Several studies discussed the long-term variations or conducted future projections of CDW in the context of climate change and explored its impact on the basal melting of Antarctic ice shelves. Dinniman et al. (2012) simulates the changes of CDW intrusion onto the western Antarctic Peninsula shelves under a shift toward positive SAM phase, and found that enhancement in westerlies and ACC can both strengthen the CDW intrusion but does not necessarily increase the CDW influx under the ice shelves, as stronger winds can also cause enhanced mixing of the warm CDW with colder water in the upper layer. Cook et al. (2016) identified dramatic retreat of Antarctic glaciers associated with warming of the mid-depth ocean temperature, which is indicative of increasing trend of the warm CDW intrusion. By conducting sensitivity numerical experiments, Dinniman et al. (2018) suggested that increased wind and lower air temperatures in the future climate scenario over the Ross Sea will enhance the on-shelf transport of CDW and the vertical mixing of mCDW on the shelf, while freshening of the Ross Sea shelf due to increased transport of ice shelf meltwater from the Amundsen Sea will reduce the on-shelf transport of CDW and vertical mixing of the mCDW. Xie et al. (2024) suggested that increased meltwater transport from the Amundsen Sea to the Ross Sea in the future will reduce eddy activities on the western Ross Sea slope and inhibit the onshore CDW intrusion, while enhance the CDW intrusion in the eastern Ross Sea by increasing the along-slope density gradient and on-shore baroclinic currents.

5 Antarctic Bottom Water

As early as during the *Challenger* expedition of 1872–1876, cold waters were observed in the deep and bottom layers of interconnected basins of the world ocean, indicating a polar origin of these waters. Waters in the bottom layers of the global ocean, with their origins from

the formation sites close to Antarctica and with temperatures below 2℃, are collectively referred to as "Antarctic Bottom Water" (Speer and Zenk, 1993; Orsi et al., 1999). In the Southern Ocean, AABW includes deep waters with potential temperatures below 0℃ (Gordon and Tchernia, 1978). Occupying much of the world ocean floor, AABW is colder than the bottom water originating from the northern source (Speer and Zenk, 1993). Mantyla and Reid (1983) documented the occupation of AABW in the global ocean, and Johnson (2008) estimated that AABW accounts for about 40% of the global ocean volume. In the Southern Ocean, AABW is defined as the water with neutral density greater than 28.27 kg/m^3 and temperature above –1.7℃ (Whitworth III et al., 1998; Orsi et al., 1999).

5.1 *AABW spatial pattern*

AABW has a quasi-circumpolar distribution, but does not appear at Drake Passage and is very thin at a few choke points, e.g., the sill of the Princess Elizabeth Trough (65°S, 80°E) and the sill located near Balleny Trough (65°S, 160°E) (Orsi et al., 1999). AABW also exists on the upper slope and outer continental shelf in some regions (Whitworth III et al., 1998).

On basin scale, AABW is the thickest in the Weddell basin, and then becomes thinner in the Weddell-Enderby basin and in the central Pacific basin (or the western part of the southeast Pacific basin), and the thinnest in the Australian-Antarctic Basin (Orsi et al., 1999). The freshest and coldest AABW is found in the Weddell Sea. Gradually, AABW becomes saltier and warmer eastward and the saltiest in the Ross Sea.

AABW exits the Southern Ocean through deep western boundary currents, replenishing the abyss of all basins to the north (except parts of the North Atlantic and Arctic Oceans). Beneath the southward flowing NADW, the northward flowing AABW upwells into the lower layer of NADW through mixing processes and returns to the south as the lower portion of NADW (Talley, 2013). In the Pacific and Indian basins, the AABW is the major contributor to the formation of Pacific Deep Water and Indian Deep Water through diffusive processes north of 32°S, with the contribution from NADW being minor and no surface sources (Talley, 2013). The AABW returns to the south in the form of Pacific Deep Water and Indian Deep Water in these two basins.

5.2 *AABW formation processes*

The formation of AABW involves processes of strong atmosphere-ocean-cryosphere interactions on a variety of scales, from small to global scale and from turbulence to millennial scale.

Two modes have been proposed to describe the formation of AABW: the shelf sea mode and the open-ocean mode (Gordon, 2014). The shelf sea mode is a primary mode under the present-day climatic conditions, and the open-ocean mode was observed to function during the mid-1970s (Gordon, 1978, 1982) and possibly at earlier times (de Lavergne et al., 2014).

5.2.1 *Shelf sea mode*

As a typical example, Fig. 5 illustrates the key processes involved in the formation of the precursors of AABW, i.e., High Salinity Shelf Water, and then DSW (Gill, 1973; Foster and Carmack, 1976; Foldvik et al., 2004; Orsi and Wiederwohl, 2009). In winter, cold and dry katabatic winds (Turner et al., 2009; Wang et al., 2021; Morrison et al., 2023) push sea ice away from ice shelf fronts or coasts. Such a process makes areas with low sea ice concentration, i.e., coastal polynyas, and

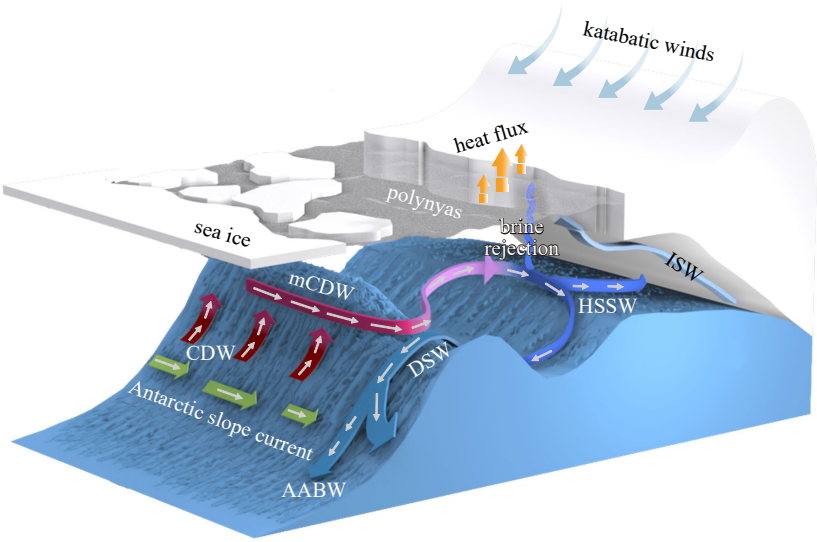


Fig. 5. Schematic of AABW formation processes (shelf sea mode). AABW: Antarctic Bottom Water; CDW: Circumpolar Deep Water; DSW: Dense Shelf Water; HSSW: High Salinity Shelf Water; ISW: Ice Shelf Water; mCDW: modified Circumpolar Deep Water.

hence strong oceanic heat losses over these polynyas. Consequently, new ice forms and is then pushed away by offshore winds, leading to persistent brine rejection that makes the surface water dense (Ohshima et al., 2022). These polynya regions are narrow, but they produce about 10% of Antarctic sea ice (Tamura et al., 2008), so they are also known as "ice factories" (Gordon and Comiso, 1988). As the mixed layer deepens, salty water in the deeper layer is entrained into the mixed layer, which could make the mixed layer further dense, forming a positive feedback. If the surface forcing is strong enough, the convection can reach a great depth or even the bottom to form HSSW (Miller et al., 2024).

HSSW can mix with some water masses on the shelf to form DSW, such as mixing with Ice Shelf Water, a mixture of melting water at the base of the ice shelf and its ambient water (Campagne et al., 2015; Williams et al., 2016; Naveira Garabato et al., 2017; Zheng et al., 2021), and mixing with mCDW (Orsi and Wiederwohl, 2009).

During the export of DSW towards the shelf break and descending over the slope, oceanic processes, such as waves (Wang et al., 2009; Jensen et al., 2013; Han et al., 2022, 2023), eddies (Stewart and Thompson, 2015; Mack et al., 2019; Spall and Price, 1998; Darelius et al., 2009; Wang et al., 2009; Nakayama et al., 2014a), and tides (MacAyeal, 1984; Padman et al., 2003; Robertson, 2005a, 2005b; Ou et al., 2009; Guan et al., 2009; Han et al., 2024), modulate the pathway and transform the properties of DSW, along with overlying atmospheric forcing (Wang et al., 2021, 2023a; Morrison et al., 2023) and the dynamic effects of bottom topography (Wåhlin et al., 2008; Muench et al., 2009; Wang et al., 2009; Nakayama et al., 2014a).

Based on analyzing chlorofluorocarbon concentrations, the circumpolar export rate of DSW was estimated as 5.4×10^6 m^3/s, which forms 8.1×10^6 m^3/s of AABW by entraining 2.7×10^6 m^3/s of CDW (Orsi et al., 2002). By analyzing shelf water budgets and natural and anthropogenic tracers, the circumpolar formation rate was estimated to be within 4.5×10^6–11×10^6 m^3/s (Weiss et al., 1979; Mensch et al., 1996; Gill, 1973; Carmack, 1977; Orsi et al., 1999, 2002; Weppernig et al., 1996; Meredith et al., 2001), as summarized in Naveira Garabato et al. (2002).

5.2.2 *Open-ocean mode*

Deep convection is a major process for the deep water formation in the North Atlantic, e.g., in the Labrador Sea, where the maximum mixed layer depth can reach about 2 000 m (Marshall and Schott, 1999; Yashayaev and Loder, 2017). Though the shelf sea mode is the dominant mode of the AABW formation for the present-day condition, deep convection did occur to produce AABW. Also, in many current-generation climate models, deep convection wildly exists in the Southern Ocean and is the major mechanism of the AABW formation (Wang and Chen, 2019).

It was observed that deep convection occurred during the mid-1970s in the Weddell Sea (Gordon, 1978, 1982). Throughout the winters of 1974–1976, a large and persistent open-ocean polynya, named as the Weddell Polynya, occurred near the Maud Rise (Gordon and Comiso, 1988). The size of the polynya was estimated to be 2×10^5–3×10^5 km^2 (Carsey, 1980). Hydrographic observations suggested that the associated deep convection reached a depth of about 4 000 m (Gordon, 1978). It was estimated that the bottom water formation rate was about 1.6×10^6–3.2×10^6 m^3/s (Gordon, 1982) using surface flux data. A modeling study suggested that the bottom water formation rate could be about 5×10^6 m^3/s (Wang et al., 2017).

5.3 *Temporal variations of DSW/AABW and drivers*

5.3.1 *Temporal variations of DSW and drivers*

Despite even much more sparse samplings in the Antarctic marginal seas, Schmidtko et al. (2014) analyzed the changes in bottom water temperature and salinity in the shelf sea regions for the period of 1975 to 2012, except for the Bellingshausen and Amundsen Seas where observations started from the 1990s. Statistically significant freshening was detected in the Ross Sea continental shelf and some narrow shelf regions between 45°E and 90°E. Warming mainly occurred in the Bellingshausen and Amundsen Seas, and slight cooling in the Weddell Sea continental shelf.

The warming in the Bellingshausen and Amundsen Seas has been attributed to the enhanced upwelling of CDW (Schmidtko et al., 2014; Turner et al., 2017). The Amundsen Sea Low has been found to be deepened (Turner et al., 2017), which might contribute to causing stronger CDW upwelling and more intrusion onto the continental shelf (Schmidtko et al., 2014). The warming in this region could enhance the basal melting of ice shelves and the retreat of the glaciers in West Antarctica (Turner et al., 2017), which was suggested to make contributions to the long-term freshening on the Ross Sea continental shelf (Jacobs et al., 2002; Jacobs and Giulivi, 2010).

However, there exists considerable interannual and decadal variability in the salinity of DSW on the Ross Sea continental shelf, featured by a decreasing trend in the past decades (Jacobs and Giulivi, 2010; Jacobs et al., 2022) and a sharp rebound since 2014 (Castagno et al., 2019; Jacobs et al., 2022; Silvano et al., 2020). Two processes have been proposed to be involved in the salinity rebound in the DSW on the Ross Sea continental shelf (Guo et al., 2020; Silvano et al., 2020). First, a reduction in the meltwater transport from the Bellingshausen and Amundsen Seas into the Ross Sea continental shelf, caused by the weakening of the slope and coastal currents, was a possible process (Guo et al., 2020). Second, the su-

perposition of positive Southern Annular Mode (SAM) and El Niño was suggested to lead to reduced sea ice transport into the Ross Sea continental shelf and hence increased sea ice production (Silvano et al., 2020).

5.3.2 *Temporal variations of AABW and drivers*

The freshening in the DSW on the Ross Sea continental shelf is presumably responsible for the freshening in the Ross Sea Bottom Water (RSBW). It is also possible that such influence could reach the Australian-Antarctic Basin.

Purkey et al. (2018) synthesized the circumpolar changes in bottom water properties (see their Fig. 7) using hydrographic data collected during 1981–2015. Freshening mainly occurred in the Ross Sea and in its immediate downstream region, the Australian-Antarctic Basin, but the signal becomes very weak in the other regions. The freshening in the RSBW was linked to the shrinking and retreat of ice shelves and glaciers in West Antarctica (e.g., Jacobs and Giulivi, 2010). As the DSW on the Ross Sea continental shelf is the precursor of the RSBW, a sharp rebound in the salinity of RSBW since 2015 was also observed (Castagno et al., 2019; Jacobs et al., 2022; Silvano et al., 2020).

Warming occurred over the circumpolar region, though stronger warming was in the Atlantic sector and weaker warming in the southeast Pacific sector. The warming was suggested to be caused by the lowering of isotherms induced by the shrinking of the bottom water volume (Purkey and Johnson, 2013). Therefore, the warming could partially originate from the freshening of the bottom water. However, the significant warming in the Atlantic sector might not be linked to the freshening, as the freshening is much less significant in the Atlantic sector than in the other sectors (Purkey and Johnson, 2013). Warming of AABW contributes to about 10% of the ocean heat uptake and 9% of thermosteric sea level rise over the globe between the 1980s and 2000s (Purkey and Johnson, 2010, 2012).

Gao et al. (2022) analyzed CTDs and profiling float profiles during 2003–2020 in the southwest Indian Ocean sector. They found significant cooling, freshening, and increasing dissolved oxygen on the continental slope off Cape Darnley Polynya, while warming, freshening, decreasing density, and increasing dissolved oxygen in the Daly Canyon. They suggested that these changes were likely caused by enhanced DSW export in Daly Canyon and subsequent entrainment of CDW.

Schmidt et al. (2023) demonstrated that there exists strong interannual variability in the formation and export of AABW by using a high-resolution ocean-sea ice model [ACCESS-OM2-01; horizontal resolution of (1/10)°]. They found that the primary driver is the strength of easterly winds: stronger easterly winds transport more sea ice into the AABW formation region, resulting in less sea ice production and hence less AABW production.

Zhou et al. (2023) reported a decrease of about 30% in the Weddell Sea Bottom Water volume during the period from around 1992 to around 2020 and the decrease in the densest classes is the largest. They attributed these changes to more than 40% decline in the sea-ice production rate over the southern Weddell continental shelf, presumably induced by increasing northerly wind trend related to the Interdecadal Pacific Oscillation and the variability in the Amundsen Sea Low.

Gunn et al. (2023) found that AABW transport weakened by about 4.0×10^6 m^3/s from 1994 to 2009 in the Australian-Antarctic Basin, corresponding to strong freshening on the continental shelf. When the freshening was reversed on the shelf between 2009 and 2018, a partial recovery of about 2.2×10^6 m^3/s was observed.

Biló et al. (2024) analyzed mooring observations and hydrographic data at 16°N and found that the shrinking in the AABW volume in the Southern Ocean affected the northward AABW transport in the North Atlantic, leading to a reduction of $(0.35 \pm 0.13) \times 10^6$ m^3/s between 2000 and 2020 below 4 500 m [mean volume transport of $(2.40 \pm 0.25) \times 10^6$ m^3/s]. Also, they found that the consequent warming of the AABW layer in the subtropical North Atlantic is about 1 (m·℃)/a averaged over this period.

5.4 *Modeling of AABW*

5.4.1 *Global models*

The AABW-driven lower cell of global overturning circulation is an essential component in the global climate system, as a result of strong interactions between the atmosphere, ocean, and cryosphere on various spatial and temporal scales. Therefore, the processes associated with AABW formation and their global impacts have to be simulated in global climate models or earth system models.

Current generation climate models have difficulties in simulating the formation processes and the export pathways of AABW, considerably reducing our confidence in properly simulating the global overturning circulation and hence climate variability. Simulated properties in AABW differ considerably from the observations, and inter-model spreads are too large, in CMIP5 (Heuzé et al., 2013). The biases have been found reduced in CMIP6, but AABW forms predominantly by the open-ocean mode in many models in the present-day conditions, rather than by the more realistic shelf sea mode (Heuzé, 2021). The poor ability of these coupled models to simulate the AABW formation processes is partially attributed to the deficiencies in representing the subpolar ocean circulations (Wang and Meredith, 2008; Wang et al., 2011; Wang, 2013; Wang and Chen, 2019).

Stand-alone ocean-sea ice models have also been used to simulate the processes involved in the formation of AABW or DSW. Wang et al. (2017) used MITgcm-ECCO2, a global coupled ocean-sea ice model forced by

JRA55 (Menemenlis et al., 2008), to investigate the formation of AABW induced by open-ocean deep convection. By intensifying the westerly winds over the Southern Ocean, open-ocean deep convection in the Weddell Sea can develop, which greatly increases the volume of AABW. By analyzing the simulations from the coupled Finite Element Sea-ice Ocean Model (FESOM) driven by the CORE-II forcing, Wang et al. (2021) examined the formation of HSSW in the Prydz Bay Polynya and the Shackleton Polynya in response to strong wind events. They found that the HSSW formation rate through the wintertime is obviously larger in those years with more persistent strong wind events.

Climate models have been applied to project the future changes in the AABW formation and transport. In a particular coupled climate model (The Community Earth System Model version 1.2.2), abrupt CO_2 doubling (734×10^{-6}) and quadrupling ($1\,468 \times 10^{-6}$) lead to decreases in sea ice production by 6%–8% and 10%–30%, respectively, which substantially freshens shelf waters along with increased precipitation, during the model integrations of 100 years (Jeong et al., 2023). As a result, CO_2 doubling weakens DSW formation by about 75%, and CO_2 quadrupling leads to a complete cessation of DSW formation. Li et al. (2023a) used a high-resolution coupled ocean-sea-ice model to conduct a transient simulation forced by a future climate under high-emissions scenario. They found that the meltwater input from the Antarctic ice sheet is mainly responsible for the shrinking of AABW and hence warming and aging of the abyssal ocean over the next 30 years.

5.4.2 *Regional models*

Regional ocean models have been used for simulating the shelf sea processes, including those based on the MITgcm (Marshall et al., 1997), a *z*-coordinate ocean model, and the Regional Ocean Modeling System (ROMS) (Shchepetkin and McWilliams, 2005), a terrain-following ocean model. By increasing the vertical resolution of the MITgcm to 10 m near the bottom and relaxing the hydrostatic assumption, periodic downslope flows of dense water are reproduced associated with the cascading processes of DSW in Cape Darnley (Nakayama et al., 2014a). MITgcm has also been used to simulate how the export of DSW breaks the PV barrier imposed by the isopycnal structure of the Antarctic Slope Front, which facilitates the eddy generation and hence the cross-slope exchange (Stewart and Thompson, 2015, 2016). The MITgcm is further coupled to a dynamic and thermodynamic sea ice model and a static thermodynamic ice shelf model to simulate the shelf sea processes in Prydz Bay (Liu et al., 2017; 2018) and in the Ross Sea (Yan et al., 2023). The seasonal cycle of the formation of DSW in the Ross Sea has been analyzed in a quantitative way, thanks to the development of the regional coupled ocean-sea ice-ice shelf model in the Ross Sea (Yan et al., 2023).

Wang et al. (2023a) found that sea ice production and DSW formation were enhanced in response to synoptic-scale and mesoscale cyclones in the western Ross Ice Shelf Polynya using a coupled ocean-sea ice-ice shelf model, based on ROMS. Also, the DSW exports through the Drygalski Trough and the Glomar Challenger Trough were in good correlation with the meridional wind. Han et al. (2022) applied an idealized model configuration of ROMS to simulate the dynamical processes of the downslope transport of DSW. They found that Topographic Rossby Waves (TRWs) can lead to oscillating downslope transport of DSW, but a steep slope does not favor the genesis of TRWs. Further, they found that the wavelength and frequency of the TRWs are constrained by the geostrophic along-slope flow speed of the DSW and by the dynamics of linear plane waves (Han et al., 2023).

6 Concluding remarks

In this article, we documented the recent advances in understanding the formation, transformation and transport of the four major water masses in the Southern Ocean — SAMW, AAIW, CDW, and AABW. These advances have considerably increased the appreciation of the critical importance of the Southern Ocean in global energy budget and hydrological cycle, carbon cycle, and sea level change.

Studies in recent decades enhance the understanding of formation, transformation and circulation of SAMW and AAIW, especially the effects of air-sea exchanges, advection, subduction, upwelling, isopycnal/diapycnal mixing, and eddy-induced processes. The comparison of historical observation data reveals that, in the past five decades, SAMW and AAIW shows statistically significant strong circumpolar shoaling, warming, and density reductions, and freshening in the southeast Pacific, southwest Atlantic, and south-central Indian Oceans. These trends are strongest just north of the ACC in the southeast Pacific and Atlantic Oceans and decrease equatorward, which indicates that signals of global warming have entered the interior ocean, carried by AAIW through its ventilation and transport in the Southern Ocean. CDW has made significant contributions to the basal melting of Antarctic ice shelves. The changes of the presence and vertical mixing of CDW on Antarctic continental shelves are affected by wind changes associated with major climate modes such as SAM and freshwater input from ice shelf melting, which can vary across different regions depending on the local dynamic environments. There is a long-term freshening trend in AABW, particularly in the Ross Sea and its downstream region. This freshening trend has been attributed to the accelerated basal melting and retreating of ice shelves and glaciers in West Antarctica. The shrinking of AABW in the Weddell Sea has also been observed and is attributed to reduced sea ice production over the southern Weddell continental shelf owing to

increasing northerly wind trend related to the Interdecadal Pacific Oscillation and the variability in the Amundsen Sea Low. The formation processes of DSW on the Antarctic shelf, the precursor of AABW, can be fairly captured in some global ocean-sea ice models or even coupled climate models. The further weakening of AABW formation has been projected in these global models, with glacial meltwater and reduced sea ice production possibly playing major roles.

Despite significant advancements in our understanding of water masses in the Southern Ocean, many research challenges remain, including still sparse spatial-temporal coverage of observational data, incomplete understanding of the formation mechanisms, and large uncertainties in model projections. Data accumulation on WOCE transects is an important basis for revealing long-term changes in these water masses. Argo and deep Argo will provide unprecedented data to study the spatiotemporal variations in these water masses. Much more *in-situ* observations beneath ice shelves by autonomous underwater vehicles or underwater gliders are needed to explore the complex interaction between the CDW inflow into ice cavities, the meltwater outflow and the circulations affected by these flows. Bathymetry and ice shelf geometry also demand much more accurate observation. To have a more comprehensive understanding of the formation and transformation mechanisms of these water masses, observations of associated meso-scale and sub-meso-scale processes are necessary, including eddies, mixing, and convection.

To improve model projections, eddy-resolving models with horizontal resolutions of 1 km or finer needed to be developed to achieve realistic representations of key processes, particularly for the shelf sea processes and ocean-ice shelf interactions. Eddies are much smaller in the Antarctic marginal seas. The first baroclinic Rossby radius is even less than one kilometer in the convection region on the continental shelf of the Ross Sea (Mack, 2017); high-resolution models are also needed to simulate the lateral export of ice shelf water by resolving the symmetric and centrifugal instability (Naveira Garabato et al., 2017). It is a challenge to directly resolve or parameterize these processes in global models. By conducting inter-model comparisons among models with different configurations, critical processes can be better understood and more faithfully simulated.

Future studies also need to strengthen interdisciplinary collaborations to collect comprehensive observational data to assess the impact of these water masses on global climate and biogeochemical dynamics. More advanced observation techniques and data analysis methods should also be developed to improve the understanding of the formation and evolution mechanisms of these water masses.

Acknowledgements

Zhaomin Wang and Chengyan Liu are grateful to Liangjun Yan for his assistance in preparing Figs 1 and 5. Ying Li is grateful to Ran Wang for providing the original map of Fig. 2. Jiuxin Shi is grateful to Wenlai Sha and Zhi Li for preparing the base map and data of Fig. 3.

References

Aoki S, Hariyama M, Mitsudera H, et al. 2007. Formation regions of Subantarctic Mode Water detected by OFES and Argo profiling floats. Geophysical Research Letters, 34(10): L10606, doi: 10.1029/2007GL029828

Biló T C, Perez R C, Dong Shenfu, et al. 2024. Weakening of the Atlantic Meridional Overturning Circulation abyssal limb in the North Atlantic. Nature Geoscience, 17(5): 419–425, doi: 10.1038/s41561-024-01422-4

Bostock H C, Sutton P J, Williams M J M, et al. 2013. Reviewing the circulation and mixing of Antarctic Intermediate Water in the South Pacific using evidence from geochemical tracers and Argo float trajectories. Deep-Sea Research Part I: Oceanographic Research Papers, 73: 84–98, doi: 10.1016/j.dsr.2012.11.007

Bryden H L, McDonagh E L, King B A, 2003. Changes in ocean water mass properties: oscillations or trends?. Science, 300(5628): 2086–2088, doi: 10.1126/science.1083980

Campagne P, Crosta X, Houssais M N, et al. 2015. Glacial ice and atmospheric forcing on the Mertz Glacier Polynya over the past 250 years. Nature Communications, 6: 6642, doi: 10.1038/ncomms7642

Carmack E C. 1977. Water characteristics of the Southern Ocean south of the Polar Front. In: Angel M, ed. A Voyage of Discovery. Oxford: Pergamon Press, 15–41

Carsey F D. 1980. Microwave observation of the Weddell Polynya. Monthly Weather Review, 108(12): 2032–2044, doi: 10.1175/1520-0493(1980)108<2032:MOOTWP>2.0.CO;2

Castagno P, Capozzi V, DiTullio G R, et al. 2019. Rebound of shelf water salinity in the Ross Sea. Nature Communications, 10(1): 5441, doi: 10.1038/s41467-019-13083-8

Castagno P, Falco P, Dinniman M S, et al. 2017. Temporal variability of the Circumpolar Deep Water inflow onto the Ross Sea continental shelf. Journal of Marine Systems, 166: 37–49, doi: 10.1016/j.jmarsys.2016.05.006

Cerovečki I, Mazloff M R. 2016. The spatiotemporal structure of diabatic processes governing the evolution of Subantarctic Mode Water in the Southern Ocean. Journal of Physical Oceanography, 46(2): 683–710, doi: 10.1175/JPO-D-14-0243.1

Cerovečki I, Meijers A J S, Mazloff M R, et al. 2019. The effects of enhanced sea ice export from the Ross sea on recent cooling and freshening of the Southeast Pacific. Journal of Climate, 32(7): 2013–2035, doi: 10.1175/JCLI-D-18-0205.1

Cerovečki I, Talley L D, Mazloff M R, et al. 2013. Subantarctic Mode Water formation, destruction, and export in the eddy-permitting Southern Ocean State Estimate. Journal

of Physical Oceanography, 43(7): 1485–1511, doi: 10.1175/JPO-D-12-0121.1

Chen Yuanjie, Zhang Zhaoru, Wang Xuezhu, et al. 2023. Interannual variations of heat budget in the lower layer of the eastern Ross Sea shelf and the forcing mechanisms in the Southern Ocean State Estimate. International Journal of Climatology, 43(11): 5055–5076, doi: 10.1002/joc.8132

Cook A J, Holland P R, Meredith M P, et al. 2016. Ocean forcing of glacier retreat in the western Antarctic Peninsula. Science, 353(6296): 283–286, doi: 10.1126/science.aae0017

Darelius E, Smedsrud L H, Østerhus S, et al. 2009. Structure and variability of the Filchner overflow plume. Tellus A, 61(3): 446–464, doi: 10.1111/j.1600-0870.2009.00391.x

Deacon G E R. 1937. The Hydrology of the Southern Ocean. London: Cambridge University Press, 3–12

de Lavergne C, Madec G, Roquet F, et al. 2017. Abyssal ocean overturning shaped by seafloor distribution. Nature, 551(7679): 181–186, doi: 10.1038/nature24472

de Lavergne C, Palter J B, Galbraith E D, et al. 2014. Cessation of deep convection in the open Southern Ocean under anthropogenic climate change. Nature Climate Change, 4(4): 278–282, doi: 10.1038/NCLIMATE2132

Depoorter M A, Bamber J L, Griggs J A, et al. 2013. Calving fluxes and basal melt rates of Antarctic ice shelves. Nature, 502(7469): 89–92, doi: 10.1038/nature12567

Dinniman M S, Klinck J M, Hofmann E E. 2012. Sensitivity of Circumpolar Deep Water transport and ice shelf basal melt along the West Antarctic Peninsula to changes in the winds. Journal of Climate, 25(14): 4799–4816, doi: 10.1175/JCLI-D-11-00307.1

Dinniman M S, Klinck J M, Hofmann E E, et al. 2018. Effects of projected changes in wind, atmospheric temperature, and freshwater inflow on the Ross Sea. Journal of Climate, 31(4): 1619–1635, doi: 10.1175/JCLI-D-17-0351.1

England M H, Godfrey J S, Hirst A C, et al. 1993. The mechanism for Antarctic Intermediate Water renewal in a world ocean model. Journal of Physical Oceanography, 23(7): 1553–1560, doi: 10.1175/1520-0485(1993)023<1553:TMFAIW>2.0.CO;2

Evans D G, Zika J D, Naveira Garabato A C, et al. 2018. The cold transit of Southern Ocean upwelling. Geophysical Research Letters, 45(24): 13386–13395, doi: 10.1029/2018GL079986

Ferrari R, Jansen M F, Adkins J F, et al. 2014. Antarctic sea ice control on ocean circulation in present and glacial climates. Proceedings of the National Academy of Sciences of the United States of America, 111(24): 8753–8758, doi: 10.1073/pnas.1323922111

Fine R A. 1993. Circulation of Antarctic intermediate water in the South Indian Ocean. Deep-Sea Research Part I: Oceanographic Research Papers, 40(10): 2021–2042, doi: 10.1016/0967-0637(93)90043-3

Foldvik A, Gammelsrød T, Østerhus S, et al. 2004. Ice shelf water overflow and bottom water formation in the southern Weddell Sea. Journal of Geophysical Research: Oceans, 109(C2): C02015

Foster T D, Carmack E C. 1976. Frontal zone mixing and Antarctic Bottom Water formation in the southern Weddell Sea. Deep-Sea Research and Oceanographic Abstracts, 23(4): 301–317, doi: 10.1016/0011-7471(76)90872-X

Frölicher T L, Sarmiento J L, Paynter D J, et al. 2015. Dominance of the Southern Ocean in anthropogenic carbon and heat uptake in CMIP5 models. Journal of Climate, 28(2): 862–886, doi: 10.1175/JCLI-D-14-00117.1

Gao Libao, Rintoul S R, Yu Weidong. 2018. Recent wind-driven change in Subantarctic Mode Water and its impact on ocean heat storage. Nature Climate Change, 8(1): 58–63, doi: 10.1038/s41558-017-0022-8

Gao Libao, Yuan Xiaojun, Cai Wenju, et al. 2024. Persistent warm-eddy transport to Antarctic ice shelves driven by enhanced summer westerlies. Nature Communications, 15: 671, doi: 10.1038/s41467-024-45010-x

Gao Libao, Zu Yongcan, Guo Guijun, et al. 2022. Recent changes and distribution of the newly-formed Cape Darnley Bottom Water, East Antarctica. Deep-Sea Research Part II: Topical Studies in Oceanography, 201: 105119, doi: 10.1016/j.dsr2.2022.105119

Gerringa L J A, Alderkamp A C, van Dijken G, et al. 2020. Dissolved trace metals in the Ross Sea. Frontiers in Marine Science, 7: 577098, doi: 10.3389/fmars.2020.577098

Gill A E. 1973. Circulation and bottom water production in the Weddell Sea. Deep-Sea Research and Oceanographic Abstracts, 20(2): 111–140, doi: 10.1016/0011-7471(73)90048-X

Gordon A L, Tchernia P. 1978. Waters of the continental margin off Adélie Coast, Antarctica. In: Hayes D E, ed. Antarctic Oceanology II: The Australian-New Zealand Sector. Washington, DC, USA: AGU, 59–69, doi: 10.1029/AR019p0059

Gordon A L. 1978. Deep Antarctic convection west of Maud Rise. Journal of Physical Oceanography, 8(4): 600–612, doi: 10.1175/1520-0485(1978)008<0600:DACWOM>2.0.CO;2

Gordon A L. 1982. Weddell deep water variability. Journal of Marine Research, 40: 199–217

Gordon A L. 2013. Bottom water formation. In: Steele J H, Thorpe S A, Turekian K K, eds. Encyclopedia of Ocean Sciences. 2nd ed. London: Academic Press, 415–421

Gordon A L. 2014. Southern Ocean polynya. Nature Climate Change, 4(4): 249–250, doi: 10.1038/nclimate2179

Gordon A L, Comiso J C. 1988. Polynyas in the Southern Ocean. Scientific American, 258(6): 90–97, doi: 10.1038/scientificamerican0688-90

Gordon A L, Weiss R F, Smethie W M Jr, et al. 1992. Thermocline and intermediate water communication between the South Atlantic and Indian Oceans. Journal of Geophysical Research: Oceans, 97(C5): 7223–7240, doi: 10.1029/92JC00485

Guan Xiaorui, Ou Hsien-Wang, Chen Dake. 2009. Tidal effect on the dense water discharge, Part 2: a numerical study. Deep-Sea Research Part II: Topical Studies in Oceanogra-

phy, 56(13–14): 884–894, doi: 10.1016/j.dsr2.2008.10.028

Gunn K L, Rintoul S R, England M H, et al. 2023. Recent reduced abyssal overturning and ventilation in the Australian Antarctic Basin. Nature Climate Change, 13(6): 537–544, doi: 10.1038/s41558-023-01667-8

Guo Guijun, Gao Libao, Shi Jiuxin. 2020. Modulation of dense shelf water salinity variability in the western Ross Sea associated with the Amundsen Sea Low. Environmental Research Letters, 16(1): 014004, doi: 10.1088/1748-9326/abc995

Guo Guijun, Gao Libao, Shi Jiuxin, et al. 2022. Wind-driven seasonal intrusion of modified Circumpolar Deep Water onto the continental shelf in Prydz Bay, East Antarctica. Journal of Geophysical Research: Oceans, 127(12): e2022JC018741, doi: 10.1029/2022JC018741

Han Xianxian, Stewart A L, Chen Dake, et al. 2022. Topographic Rossby wave-modulated oscillations of dense overflows. Journal of Geophysical Research: Oceans, 127(9): e2022JC018702, doi: 10.1029/2022JC018702

Han Xianxian, Stewart A L, Chen Dake, et al. 2023. Controls of topographic Rossby wave properties and downslope transport in dense overflows. Journal of Physical Oceanography, 53(7): 1805–1820, doi: 10.1175/JPO-D-22-0237.1

Han Xianxian, Stewart A L, Chen Dake, et al. 2024. Circum-Antarctic bottom water formation mediated by tides and topographic waves. Nature Communications, 15(1): 2049, doi: 10.1038/s41467-024-46086-1

Hanawa K, Talley L D. 2001. Mode waters. International Geophysics, 77: 373–386, doi: 10.1016/S0074-6142(01)80129-7

Hartin C A, Fine R A, Sloyan B M, et al. 2011. Formation rates of Subantarctic Mode Water and Antarctic Intermediate Water within the South Pacific. Deep-Sea Research Part I: Oceanographic Research Papers, 58(5): 524–534, doi: 10.1016/j.dsr.2011.02.010

Herraiz-Borreguero L, Rintoul S R. 2010. Subantarctic Mode Water variability influenced by mesoscale eddies south of Tasmania. Journal of Geophysical Research: Oceans, 115(C4): C04004, doi: 10.1029/2008JC005146

Herraiz-Borreguero L, Rintoul S R. 2011. Subantarctic Mode Water: distribution and circulation. Ocean Dynamics, 61(1): 103–126, doi: 10.1007/s10236-010-0352-9

Heuzé C. 2021. Antarctic Bottom Water and North Atlantic Deep Water in CMIP6 models. Ocean Science, 17(1): 59–90, doi: 10.5194/os-17-59-2021

Heuzé C, Heywood K J, Stevens D P, et al. 2013. Southern Ocean bottom water characteristics in CMIP5 models. Geophysical Research Letters, 40(7): 1409–1414, doi: 10.1002/grl.50287

Holzer M, DeVries T, de Lavergne C. 2021. Diffusion controls the ventilation of a Pacific Shadow Zone above abyssal overturning. Nature Communications, 12(1): 4348, doi: 10.1038/s41467-021-24648-x

Hong Yu, Du Yan, Qu Tangdong, et al. 2020. Variability of the Subantarctic Mode Water volume in the South Indian Ocean during 2004–2018. Geophysical Research Letters, 47(10): e2020GL087830, doi: 10.1029/2020gl087830

Iudicone D, Rodgers K B, Stendardo I, et al. 2011. Water masses as a unifying framework for understanding the Southern Ocean Carbon Cycle. Biogeosciences, 8(5): 1031–1052, doi: 10.5194/bg-8-1031-2011

Jacobs S S, Giulivi C F. 2010. Large multidecadal salinity trends near the Pacific-Antarctic continental margin. Journal of Climate, 23(7): 4508–4524, doi: 10.1175/2010JCLI3284.1

Jacobs S S, Giulivi C F, Dutrieux P. 2022. Persistent Ross Sea freshening from imbalance West Antarctic ice shelf melting. Journal of Geophysical Research: Oceans, 127(3): e2021JC017808, doi: 10.1029/2021JC017808

Jacobs S S, Giulivi C F, Mele P A. 2002. Freshening of the Ross Sea during the late 20th century. Science, 297(5580): 386–389, doi: 10.1126/science.1069574

Jensen M F, Fer I, Darelius E. 2013. Low frequency variability on the continental slope of the southern Weddell Sea. Journal of Geophysical Research: Oceans, 118(9): 4256–4272, doi: 10.1002/jgrc.20309

Jeong H, Lee S S, Park H S, et al. 2023. Future changes in Antarctic coastal polynyas and bottom water formation simulated by a high-resolution coupled model. Communications Earth & Environment, 4: 490

Jing Wandi, Luo Yiyong. 2021. Volume budget of Subantarctic Mode Water in the Southern Ocean from an ocean general circulation model. Journal of Geophysical Research: Oceans, 126(10): e2020JC017040

Jing Wandi, Luo Yiyong, Zhang Ronghua. 2024. Low-frequency variability of upper-ocean temperature in the Central Pacific Subantarctic Mode Water formation region since the 1980s. Climate Dynamics, 62(6): 1–14, doi: 10.1007/s00382-024-07134-0

Johnson G C. 2008. Quantifying Antarctic bottom water and North Atlantic deep water volumes. Journal of Geophysical Research: Oceans, 113(C5): C05027, doi: 10.1029/2007JC004477

Klinck J M, Dinniman M S. 2010. Exchange across the shelf break at high southern latitudes. Ocean Science, 6(2): 513–524, doi: 10.5194/os-6-513-2010

Kobayashi T, Mizuno K, Suga T. 2012. Long-term variations of surface and intermediate waters in the southern Indian Ocean along 32°S. Journal of Oceanography, 68(2): 243–265, doi: 10.1007/S10872-011-0093-5

Li Qian, England M H, Hogg A M, et al. 2023a. Abyssal ocean overturning slowdown and warming driven by Antarctic meltwater. Nature, 615(7954): 841–847, doi: 10.1038/s41586-023-05762-w

Li Zhi, England M H, Groeskamp S, et al. 2021. The origin and fate of Subantarctic Mode Water in the Southern Ocean. Journal of Physical Oceanography, 51(9): 2951–2972, doi: 10.1175/JPO-D-20-0174.1

Li Zhi, England M H, Groeskamp S. 2023b. Recent acceleration in global ocean heat accumulation by mode and intermediate waters. Nature Communications, 14(1): 6888, doi: 10.1038/s41467-023-42468-z

Li Zhi, Groeskamp S, Cerovečki I, et al. 2022. The origin and

fate of Antarctic Intermediate Water in the Southern Ocean. Journal of Physical Oceanography, 52(11): 2873–2890, doi: 10.1175/JPO-D-21-0221.1

Liu Chengyan, Wang Zhaomin, Cheng Chen, et al. 2017. Modeling modified Circumpolar Deep Water intrusions onto the Prydz Bay continental shelf, East Antarctica. Journal of Geophysical Research: Oceans, 122(7): 5198–5217, doi: 10.1002/2016JC012336

Liu Chengyan, Wang Zhaomin, Cheng Chen, et al. 2018. On the modified Circumpolar Deep Water upwelling over the Four Ladies Bank in Prydz Bay, East Antarctica. Journal of Geophysical Research: Oceans, 123(11): 7819–7838, doi: 10.1029/2018JC014026

Liu Chengyan, Wang Zhaomin, Liang Xi, et al. 2022. Topography-mediated transport of warm deep water across the continental shelf slope, East Antarctica. Journal of Physical Oceanography, 52(6): 1295–1314

Lumpkin R, Speer K. 2007. Global ocean meridional overturning. Journal of Physical Oceanography, 37(10): 2550–2562, doi: 10.1175/JPO3130.1

MacAyeal D R. 1984. Numerical simulations of the Ross Sea tides. Journal of Geophysical Research: Oceans, 89(C1): 607–615, doi: 10.1029/JC089iC01p00607

Mack S L. 2017. Influence of tides and mesoscale eddies in the Ross Sea [dissertation]. Norfolk: Old Dominion University

Mack S L, Dinniman M S, Klinck J M, et al. 2019. Modeling ocean eddies on Antarctica's cold water continental shelves and their effects on ice shelf basal melting. Journal of Geophysical Research: Oceans, 124(7): 5067–5084, doi: 10.1029/2018JC014688

Mantyla A W, Reid J L. 1983. Abyssal characteristics of the World Ocean waters. Deep-Sea Research Part A. Oceanographic Research Papers, 30(8): 805–833

Marinov I, Gnanadesikan A, Toggweiler J R, et al. 2006. The Southern Ocean biogeochemical divide. Nature, 441(7096): 964–967, doi: 10.1038/nature04883

Marsh R, Nurser A J G, Megann A P, et al. 2000. Water mass transformation in the Southern Ocean of a global isopycnal coordinate GCM. Journal of Physical Oceanography, 30(5): 1013–1045, doi: 10.1175/1520-0485(2000)030<1013:WMTITS>2.0.CO;2

Marshall J, Adcroft A, Hill C, et al. 1997. A finite-volume, incompressible Navier Stokes model for studies of the ocean on parallel computers. Journal of Geophysical Research: Oceans, 102(C3): 5753–5766, doi: 10.1029/96JC02775

Marshall J, Schott F. 1999. Open-ocean convection: observations, theory, and models. Reviews of Geophysics, 37(1): 1–64, doi: 10.1029/98RG02739

Marzocchi A, Jansen M F. 2019. Global cooling linked to increased glacial carbon storage via changes in Antarctic sea ice. Nature Geoscience, 12(12): 1001–1005, doi: 10.1038/s41561-019-0466-8

McCarthy G, McDonagh E, King B. 2011. Decadal variability of thermocline and intermediate waters at 24°S in the South Atlantic. Journal of Physical Oceanography, 41(1): 157–165, doi: 10.1175/2010JPO4467.1

McCartney M S. 1977. Subantarctic mode water. In: Angel M V, ed. A Voyage of Discovery: George Deacon 70th Anniversary Volume. Supplement to Deep-Sea Research. Oxford, UK: Pergamon Press, 103–119

Meijers A J S, Cerovečki I, King B A, et al. 2019. A see-saw in Pacific Subantarctic Mode Water formation driven by atmospheric modes. Geophysical Research Letters, 46(22): 13152–13160, doi: 10.1029/2019GL085280

Menemenlis D, Campin J M, Heimbach P, et al. 2008. ECCO2: high resolution global ocean and sea ice data synthesis. Mercator Ocean Quarterly Newsletter, 31: 13–21

Mensch M, Bayer R, Bullister J L, et al. 1996. The distribution of tritium and CFCs in the Weddell Sea during the mid-1980s. Progress in Oceanography, 38(4): 377–415, doi: 10.1016/S0079-6611(97)00007-4

Meredith M P, Watson A J, van Scoy K A, et al. 2001. Chlorofluorocarbon-derived formation rates of the deep and bottom waters of the Weddell Sea. Journal of Geophysical Research: Oceans, 106(C2): 2899–2919, doi: 10.1029/2000JC900119

Miller U K, Zappa C J, Gordon A L, et al. 2024. High Salinity Shelf Water production rates in Terra Nova Bay, Ross Sea from high-resolution salinity observations. Nature Communications, 15(1): 373, doi: 10.1038/s41467-023-43880-1

Morlighem M, Rignot E, Binder T, et al. 2020. Deep glacial troughs and stabilizing ridges unveiled beneath the margins of the Antarctic ice sheet. Nature Geoscience, 13(2): 132–137, doi: 10.1038/s41561-019-0510-8

Morrison A K, Hogg A M, England M H, et al. 2020. Warm Circumpolar Deep Water transport toward Antarctica driven by local dense water export in canyons. Science Advances, 6(18): eaav2516

Morrison A K, Huneke W G C, Neme J, et al. 2023. Sensitivity of Antarctic shelf waters and abyssal overturning to local winds. Journal of Climate, 36(18): 6465–6479, doi: 10.1175/JCLI-D-22-0858.1

Muench R, Padman L, Gordon A, et al. 2009. A dense water outflow from the Ross Sea, Antarctica: mixing and the contribution of tides. Journal of Marine Systems, 77(4): 369–387, doi: 10.1016/j.jmarsys.2008.11.003

Nakayama Y, Ohshima K I, Matsumura Y, et al. 2014a. A numerical investigation of formation and variability of Antarctic Bottom Water off Cape Darnley, East Antarctica. Journal of Physical Oceanography, 44(11): 2921–2937, doi: 10.1175/JPO-D-14-0069.1

Nakayama Y, Timmermann R, Rodehacke C B, et al. 2014b. Modeling the spreading of glacial meltwater from the Amundsen and Bellingshausen Seas. Geophysical Research Letters, 41(22): 7942–7949, doi: 10.1002/2014GL061600

Naveira Garabato A C, Forryan A, Dutrieux P, et al. 2017. Vigorous lateral export of the meltwater outflow from beneath an Antarctic ice shelf. Nature, 542(7640): 219–222, doi: 10.1038/nature20825

Naveira Garabato A C, Jullion L, Stevens D P, et al. 2009. Variability of Subantarctic Mode Water and Antarctic Interme-

diate Water in the Drake Passage during the late-twentieth and early-twenty-first centuries. Journal of Climate, 22(13): 3661–3688, doi: 10.1175/2009jcli2621.1

Naveira Garabato A C, McDonagh E L, Stevens D P, et al. 2002. On the export of Antarctic bottom water from the Weddell Sea. Deep-Sea Research Part II: Topical Studies in Oceanography, 49(21): 4715–4742, doi: 10.1016/S0967-0645(02)00156-X

Ohshima K I, Fukamachi Y, Ito M, et al. 2022. Dominant frazil ice production in the Cape Darnley polynya leading to Antarctic Bottom Water formation. Science Advances, 8(42): eadc9174, doi: 10.1126/sciadv.adc9174

Ong E Q Y, Doddridge E, Constantinou N C, et al. 2024. Intrinsically episodic Antarctic shelf intrusions of circumpolar deep water via canyons. Journal of Physical Oceanography, 54(5): 1195–1210, doi: 10.1175/JPO-D-23-0067.1

Orsi A H, Johnson G C, Bullister J L. 1999. Circulation, mixing, and production of Antarctic bottom water. Progress in Oceanography, 43(1): 55–109, doi: 10.1016/S0079-6611(99)00004-X

Orsi A H, Smethie W M Jr, Bullister J L. 2002. On the total input of Antarctic waters to the deep ocean: a preliminary estimate from chlorofluorocarbon measurements. Journal of Geophysical Research: Oceans, 107(C8): 31-1–31-14

Orsi A H, Whitworth T, Nowlin W D. 1995. On the meridional extent and fronts of the Antarctic Circumpolar Current. Deep-Sea Research Part I: Oceanographic Research Papers, 42(5): 641–673, doi: 10.1016/0967-0637(95)00021-W

Orsi A H, Wiederwohl C L. 2009. A recount of Ross Sea waters. Deep-Sea Research Part II: Topical Studies in Oceanography, 56(13–14): 778–795, doi: 10.1016/j.dsr2.2008.10.033

Ou H W, Guan Xiaorui, Chen Dake. 2009. Tidal effect on the dense water discharge, Part 1: Analytical model. Deep-Sea Research Part II: Topical Studies in Oceanography, 56(13–14): 874–883, doi: 10.1016/j.dsr2.2008.10.031

Padman L, Erofeeva S, Joughin I. 2003. Tides of the Ross Sea and Ross Ice Shelf cavity. Antarctic Science, 15(1): 31–40, doi: 10.1017/S0954102003001032

Palóczy A, McClean J L, Gille S T, et al. 2020. The large-scale vorticity balance of the Antarctic continental margin in a fine-resolution global simulation. Journal of Physical Oceanography, 50(8): 2173–2188, doi: 10.1175/JPO-D-19-0307.1

Piola A R, Georgi D T. 1982. Circumpolar properties of Antarctic Intermediate Water and Subantarctic Mode Water. Deep-Sea Research Part A. Oceanographic Research Papers, 29(6): 687–711

Portela E, Kolodziejczyk N, Maes C, et al. 2020. Interior water-mass variability in the southern Hemisphere oceans during the last decade. Journal of Physical Oceanography, 50(2): 361–381, doi: 10.1175/jpo-d-19-0128.1

Purkey S G, Johnson G C. 2010. Warming of global abyssal and deep Southern Ocean waters between the 1990s and 2000s: Contributions to global heat and sea level rise budgets. Journal of Climate, 23(23): 6336–6351, doi: 10.1175/2010JCLI3682.1

Purkey S G, Johnson G C. 2012. Global contraction of Antarctic Bottom Water between the 1980s and 2000s. Journal of Climate, 25(17): 5830–5844, doi: 10.1175/JCLI-D-11-00612.1

Purkey S G, Johnson G C. 2013. Antarctic Bottom Water warming and freshening: Contributions to sea level rise, ocean freshwater budgets, and global heat gain. Journal of Climate, 26(16): 6105–6122, doi: 10.1175/JCLI-D-12-00834.1

Purkey S G, Smethie W M Jr, Gebbie G, et al. 2018. A synoptic view of the ventilation and circulation of Antarctic Bottom Water from chlorofluorocarbons and natural tracers. Annual Review of Marine Science, 10: 503–527, doi: 10.1146/annurev-marine-121916-063414

Qiu Zishan, Lan Jian, Wei Zexun, et al. 2024. Changes in spreading of Southeast Indian subantarctic mode water during Argo period. Journal of Geophysical Research: Oceans, 129(6): e2024JC020980, doi: 10.1029/2024JC020980

Qiu Zishan, Wei Zexun, Nie Xunwei, et al. 2021. Southeast Indian Subantarctic mode water in the CMIP6 coupled models. Journal of Geophysical Research: Oceans, 126(7): e2020JC016872, doi: 10.1029/2020JC016872

Qu Tangdong, Gao Shan, Fine R A. 2020. Variability of the Sub-Antarctic Mode Water subduction rate during the Argo period. Geophysical Research Letters, 47(13): e2020GL088248, doi: 10.1029/2020GL088248

Robertson R. 2005a. Baroclinic and barotropic tides in the Ross Sea. Antarctic Science, 17(1): 107–120, doi: 10.1017/S0954102005002506

Robertson R. 2005b. Baroclinic and barotropic tides in the Weddell Sea. Antarctic Science, 17(3): 461–474, doi: 10.1017/S0954102005002890

Rodriguez A R, Mazloff M R, Gille S T. 2016. An oceanic heat transport pathway to the Amundsen Sea Embayment. Journal of Geophysical Research: Oceans, 121(5): 3337–3349, doi: 10.1002/2015JC011402

Roemmich D, Church J, Gilson J, et al. 2015. Unabated planetary warming and its ocean structure since 2006. Nature Climate Change, 5(3): 240–245, doi: 10.1038/nclimate2513

Saenko O A, Weaver A J, England M H. 2003. A region of enhanced northward Antarctic intermediate water transport in a coupled climate mode. Journal of Physical Oceanography, 33(7): 1528–1535, doi: 10.1175/1520-0485(2003)033<1528:AROENA>2.0.CO;2

Sallée J B, Speer K, Rintoul S, et al. 2010. Southern Ocean thermocline ventilation. Journal of Physical Oceanography, 40(3): 509–529, doi: 10.1175/2009JPO4291.1

Sallée J B, Wienders N, Speer K, et al. 2006. Formation of sub-Antarctic Mode Water in the southeastern Indian Ocean. Ocean Dynamics, 56(5): 525–542

Sanders R N C, Meijers A J S, Holland P R, et al. 2023. Sea ice-driven variability in the Pacific subantarctic mode water formation regions. Journal of Geophysical Research: Oceans, 128(12): e2023JC020006, doi: 10.1029/2023JC

020006

Santoso A, England M H. 2004. Antarctic Intermediate Water circulation and variability in a coupled climate model. Journal of Physical Oceanography, 34(10): 2160–2179, doi: 10.1175/1520-0485(2004)034<2160:AIWCAV>2.0.CO;2

Sarmiento J L. 2006. Ocean Biogeochemical Dynamics. Princeton: Princeton University Press

Sarmiento J L, Gruber N, Brzezinski M A, et al. 2004. High-latitude controls of thermocline nutrients and low latitude biological productivity. Nature, 427(6969): 56–60, doi: 10.1038/nature02127

Schmidt C, Morrison A K, England M H. 2023. Wind- and sea-ice–driven interannual variability of Antarctic Bottom Water formation. Journal of Geophysical Research: Oceans, 128(6): e2023JC019774, doi: 10.1029/2023JC019774

Schmidtko S, Heywood K J, Thompson A F, et al. 2014. Multidecadal warming of Antarctic waters. Science, 346(6214): 1227–1231, doi: 10.1126/science.1256117

Schmidtko S, Johnson G C. 2012. Multidecadal warming and shoaling of Antarctic Intermediate Water. Journal of Climate, 25(1): 207–221, doi: 10.1175/JCLI-D-11-00021.1

Shchepetkin A F, McWilliams J C. 2005. The regional oceanic modeling system (ROMS): a split-explicit, free-surface, topography-following-coordinate oceanic model. Ocean Modelling, 9(4): 347–404, doi: 10.1016/j.ocemod.2004.08.002

Sigman D M, Boyle E A. 2000. Glacial/interglacial variations in atmospheric carbon dioxide. Nature, 407(6806): 859–869, doi: 10.1038/35038000

Silvano A, Foppert A, Rintoul S R, et al. 2020. Recent recovery of Antarctic Bottom Water formation in the Ross Sea driven by climate anomalies. Nature Geoscience, 13(12): 780–786, doi: 10.1038/s41561-020-00655-3

Sloyan B M, Rintoul S R. 2001. The Southern Ocean limb of the global deep overturning circulation. Journal of Physical Oceanography, 31(1): 143–173, doi: 10.1175/1520-0485(2001)031<0143:TSOLOT>2.0.CO;2

Sørensen J V T, Ribbe J, Shaffer G. 2001. Antarctic intermediate water mass formation in ocean general circulation models. Journal of Physical Oceanography, 31(11): 3295–3311, doi: 10.1175/1520-0485(2001)031<3295:AIWMFI>2.0.CO;2

Spall M A, Price J F. 1998. Mesoscale variability in Denmark Strait: the PV outflow hypothesis. Journal of Physical Oceanography, 28(8): 1598–1623, doi: 10.1175/1520-0485(1998)028<1598:MVIDST>2.0.CO;2

Speer K G, Zenk W. 1993. The flow of Antarctic bottom water into the Brazil Basin. Journal of Physical Oceanography, 23(12): 2667–2682, doi: 10.1175/1520-0485(1993)023<2667:TFOABW>2.0.CO;2

Stewart A L, Klocker A, Menemenlis D. 2018. Circum-Antarctic shoreward heat transport derived from an eddy- and tide-resolving simulation. Geophysical Research Letters, 45(2): 834–845, doi: 10.1002/2017GL075677

Stewart A L, Thompson A F. 2015. Eddy-mediated transport of warm Circumpolar Deep Water across the Antarctic shelf break. Geophysical Research Letters, 42(2): 432–440, doi: 10.1002/2014GL062281

Stewart A L, Thompson A F. 2016. Eddy generation and jet formation via dense water outflows across the Antarctic continental slope. Journal of Physical Oceanography, 46(12): 3729–3750, doi: 10.1175/JPO-D-16-0145.1

St-Laurent P, Klinck J M, Dinniman M S. 2013. On the role of coastal troughs in the circulation of warm circumpolar deep water on Antarctic shelves. Journal of Physical Oceanography, 43(1): 51–64, doi: 10.1175/JPO-D-11-0237.1

Talley L D. 1996. Antarctic intermediate water in the South Atlantic. In: Wefer G, Berger W H, Siedler G, et al, eds. The South Atlantic: Present and Past Circulation. Berlin: Springer, 219–238

Talley L D. 2013. Closure of the global overturning circulation through the Indian, Pacific, and Southern Oceans: Schematics and transports. Oceanography, 26(1): 80–97, doi: 10.5670/oceanog.2013.07

Talley L D, Pickard G L, Emery W J, et al. 2011. Descriptive Physical Oceanography: An Introduction. 6th ed. Amsterdam: Elsevier, 560

Tamsitt V, Abernathey R P, Mazloff M R, et al. 2018. Transformation of deep water masses along Lagrangian upwelling pathways in the Southern Ocean. Journal of Geophysical Research: Oceans, 123(3): 1994–2017, doi: 10.1002/2017JC013409

Tamsitt V, Drake H F, Morrison A K, et al. 2017. Spiraling pathways of global deep waters to the surface of the Southern Ocean. Nature Communications, 8(1): 172, doi: 10.1038/s41467-017-00197-0

Tamura T, Ohshima K I, Nihashi S. 2008. Mapping of sea ice production for Antarctic coastal polynyas. Geophysical Research Letters, 35(7): L07606

Thompson A F, Stewart A L, Spence P, et al. 2018. The Antarctic Slope Current in a changing climate. Reviews of Geophysics, 56(4): 741–770, doi: 10.1029/2018RG000624

Turner J, Chenoli S N, abu Samah A, et al. 2009. Strong wind events in the Antarctic. Journal of Geophysical Research: Atmospheres, 114(D18): D18103, doi: 10.1029/2008JD011642

Turner J, Orr A, Gudmundsson G H, et al. 2017. Atmosphere-ocean-ice interactions in the Amundsen Sea embayment, West Antarctica. Reviews of Geophysics, 55(1): 235–276, doi: 10.1002/2016RG000532

Vidya P J, Ravichandran M, Subeesh M P, et al. 2020. Global warming hiatus contributed weakening of the Mascarene High in the Southern Indian Ocean. Scientific Reports, 10(1): 3255, doi: 10.1038/s41598-020-59964-7

Wåhlin A K, Darelius E, Cenedese C, et al. 2008. Laboratory observations of enhanced entrainment in dense overflows in the presence of submarine canyons and ridges. Deep-Sea Research Part I: Oceanographic Research Papers, 55(6): 737–750, doi: 10.1016/j.dsr.2008.02.007

Wang Zhaomin. 2013. On the response of Southern Hemisphere subpolar gyres to climate change in coupled climate models. Journal of Geophysical Research: Oceans, 118(3): 1070–1086, doi: 10.1002/jgrc.20111

Wang Zhaomin, Chen Dake. 2019. Polar climate system modeling in China: Recent progress and future challenges. Science China: Earth Sciences, 62(7): 1076–1091, doi: 10.1007/s11430-018-9355-2

Wang Qiang, Danilov S, Hellmer H, et al. 2013. Enhanced cross-shelf exchange by tides in the western Ross Sea. Geophysical Research Letters, 40(21): 5735–5739, doi: 10.1002/2013GL058207

Wang Qiang, Danilov S, Schröter J. 2009. Bottom water formation in the southern Weddell Sea and the influence of submarine ridges: idealized numerical simulations. Ocean Modelling, 28(1–3): 50–59, doi: 10.1016/j.ocemod.2008.08.003

Wang Zhaomin, Kuhlbrodt T, Meredith M P. 2011. On the response of the Antarctic Circumpolar Current transport to climate change in coupled climate models. Journal of Geophysical Research, 116(C8): C08011, doi: 10.1029/2010jc006757

Wang Zhaomin, Meredith M P. 2008. Density-driven Southern Hemisphere subpolar gyres in coupled climate models. Geophysical Research Letters, 35(14): L14608, doi: 10.1029/2008GL034344

Wang Ran, Nan Feng, Yu Fei, et al. 2022. Subantarctic mode water variations in the three Southern Hemisphere ocean basins during 2004–2019. Journal of Geophysical Research: Oceans, 127(7): e2021JC017906, doi: 10.1029/2021JC017906

Wang Xiaoqiao, Zhang Zhaoru, Dinniman M S, et al. 2023a. The response of sea ice and high-salinity shelf water in the Ross Ice Shelf Polynya to cyclonic atmosphere circulations. The Cryosphere, 17(3): 1107–1126, doi: 10.5194/tc-17-1107-2023

Wang Xiaoqiao, Zhang Zhaoru, Wang Xuezhu, et al. 2021. Impacts of strong wind events on sea ice and water mass properties in Antarctic coastal polynyas. Climate Dynamics, 57(11–12): 3505–3528, doi: 10.1007/s00382-021-05878-7

Wang Chuning, Zhang Zhaoru, Zhong Yisen, et al. 2024. A model study of buoyancy driven cross-isobath transport over the Ross Sea continental shelf break. Journal of Geophysical Research: Oceans, 129(1): e2023JC020078, doi: 10.1029/2023JC020078

Wang Yufei, Zhou Meng, Zhang Zhaoru, et al. 2023b. Seasonal variations in Circumpolar Deep Water intrusions into the Ross Sea continental shelf. Frontiers in Marine Science, 10: 1020791, doi: 10.3389/fmars.2023.1020791

Wang Zhaomin, Wu Yang, Lin Xia, et al. 2017. Impacts of open-ocean deep convection in the Weddell Sea on coastal and bottom water temperature. Climate Dynamics, 48(9): 2967–2981, doi: 10.1007/s00382-016-3244-y

Weiss R F, Östlund H G, Craig H. 1979. Geochemical studies of the Weddell Sea. Deep-Sea Research Part A. Oceanographic Research Papers, 26(10): 1093–1120

Weppernig R, Schlosser P, Khatiwala S, et al. 1996. Isotope data from Ice Station Weddell: Implications for deep water formation in the Weddell Sea. Journal of Geophysical Research: Oceans, 101(C11): 25723–25739, doi: 10.1029/96JC01895

Whitworth III T, Orsi A H, Kim S J, et al. 1998. Water masses and mixing near the Antarctic Circumpolar Front. In: Jacobs S S, Weiss R F, eds. Ocean, Ice, and Atmosphere: Interactions at the Antarctic Continental Margin. Washington: American Geophysical Union

Williams G D, Herraiz-Borreguero L, Roquet F, et al. 2016. The suppression of Antarctic bottom water formation by melting ice shelves in Prydz Bay. Nature Communications, 7(1): 12577, doi: 10.1038/ncomms12577

Wong A P S. 2005. Subantarctic Mode Water and Antarctic Intermediate Water in the South Indian Ocean based on profiling float data 2000–2004. Journal of Marine Research, 63(4): 789–812, doi: 10.1357/0022240054663196

Wong A P S, Bindoff N L, Church J A. 1999. Large-scale freshening of intermediate waters in the Pacific and Indian Oceans. Nature, 400(6743): 440–443, doi: 10.1038/22733

Wong A P S, Bindoff N L, Church J A. 2001. Freshwater and heat changes in the North and South Pacific Oceans between the 1960s and 1985–94. Journal of Climate, 14(7): 1613–1633, doi: 10.1175/1520-0442(2001)014<1613:FAHCIT>2.0.CO;2

Xia Xingyue, Hong Yu, Du Yan, et al. 2022. Three types of Antarctic Intermediate Water revealed by a machine learning approach. Geophysical Research Letters, 49(21): e2022GL099445, doi: 10.1029/2022GL099445

Xie Chunhu, Shi Jiuxin, Sun Yongming, et al. 2023. Modified circumpolar deep water inflow to the Dotson-Getz trough in the summers of 2020 and 2022. Advances in Polar Science, 34(2): 80–90

Xie Chuan, Zhang Zhaoru, Chen Yuanjie, et al. 2024. The response of ross sea shelf water properties to enhanced Amundsen Sea ice shelf melting. Journal of Geophysical Research: Oceans, 129(7): e2024JC020919, doi: 10.1029/2024JC020919

Xu Lixiao, Ding Yang, Xie Shangping. 2021. Buoyancy and wind driven changes in Subantarctic Mode Water during 2004–2019. Geophysical Research Letters, 48(8): e2021GL092511, doi: 10.1029/2021GL092511

Yan Liangjun, Wang Zhaomin, Liu Chengyan, et al. 2023. The salinity budget of the Ross Sea continental shelf, Antarctica. Journal of Geophysical Research: Oceans, 128(3): e2022JC018979, doi: 10.1029/2022JC018979

Yang Xiaoyi, He Zhigang. 2014. Decadal change of Antarctic Intermediate Water in the region of Brazil and Malvinas confluence. Deep-Sea Research Part I: Oceanographic Research Papers, 88: 1–7, doi: 10.1016/j.dsr.2014.02.007

Yao Wenjun, Shi Jiuxin. 2017. Pacific-Indian interocean circulation of the Antarctic Intermediate Water around South Australia. Acta Oceanologica Sinica, 36(7): 4–14, doi: 10.1007/s13131-017-1078-z

Yao Wenjun, Shi Jiuxin, Zhao Xiaolong. 2017. Freshening of Antarctic intermediate water in the South Atlantic Ocean in 2005–2014. Ocean Science, 13(4): 521–530, doi: 10.5194/os-13-521-2017

Yashayaev I, Loder J W. 2017. Further intensification of deep convection in the Labrador Sea in 2016. Geophysical Research Letters, 44(3): 1429–1438, doi: 10.1002/2016GL071668

Zhang Ying, Du Yan, Qu Tangdong, et al. 2021. Changes in the Subantarctic Mode Water properties and spiciness in the southern Indian Ocean based on Argo observations. Journal of Physical Oceanography, 51(7): 2203–2221, doi: 10.1175/JPO-D-20-0254.1

Zhang Zhaoru, Hofmann E E, Dinniman M S, et al. 2020. Linkage of the physical environments in the northern Antarctic Peninsula region to the Southern Annular Mode and the implications for the phytoplankton production. Progress in Oceanography, 188: 102416, doi: 10.1016/j.pocean.2020.102416

Zhang Jinjuan, Luo Yiyong, Jing Wandi, et al. 2023. Volume budget of Antarctic Intermediate Water in the Southern Ocean from an eddy-resolving ocean simulation. Atmosphere-Ocean, 61(2): 94–104, doi: 10.1080/07055900.2022.2118568

Zheng Yixi, Heywood K J, Webber B G M, et al. 2021. Winter seal-based observations reveal glacial meltwater surfacing in the southeastern Amundsen Sea. Communications Earth & Environment, 2: 40

Zhou Shenjie, Meijers A J S, Meredith M P, et al. 2023. Slowdown of Antarctic Bottom Water export driven by climatic wind and sea-ice changes. Nature Climate Change, 13(7): 701–709, doi: 10.1038/s41558-023-01695-4